Vol. 89: 1–22, 2023
https://doi.org/10.3354/ame01994

AQUATIC MICROBIAL ECOLOGY
Aquat Microb Ecol

Published March 23

Interaction between temperature and salinity stress on the physiology of *Dinophysis* spp. and *Alexandrium minutum*: implications for niche range and blooming patterns

Pilar Rial[1,2,*,#], Marta Sixto[1,2,#], José Antonio Vázquez[3], Beatriz Reguera[1], Rosa I. Figueroa[1], Pilar Riobó[3], Francisco Rodríguez[1]

[1]Centro Oceanográfico de Vigo, Instituto Español de Oceanografía (IEO-CSIC), Subida a Radio Faro 50-52, 36390 Vigo, Spain
[2]Campus do Mar, Facultad de Ciencias del Mar, Universidad de Vigo, 36311 Vigo, Spain
[3]Instituto de Investigaciones Marinas, Consejo Superior de Investigaciones Científicas (IIM-CSIC), 36208 Vigo, Spain

ABSTRACT: Abrupt changes in environmental conditions in estuaries and coastal waters have direct (physiological) and indirect (through changes in water column stability) effects on planktonic microalgae. Understanding and quantifying these effects is important to improve harmful algal bloom predictive models. *Dinophysis* spp. (*D. acuminata*, *D. acuta* and *D. caudata*) and *Alexandrium minutum* produce toxins that are transferred through the food web (particulate) by filter feeders and also released in the seawater. These dinoflagellates cause lengthy harvesting bans in European aquaculture sites and affect marine life. The 4 species were exposed to different combinations of temperature (T) and salinity (S) to investigate their short-term response (days) to and their recovery (weeks) from T/S stress. *Dinophysis* species showed varying capacities to deal with sudden changes in S, from the most resilient *D. acuminata*, equally affected by T and S stress, to the less tolerant *D. acuta*, and in particular *D. caudata*, more affected by S than T stress. The euryhaline *A. minutum* thrived under all the T/S combinations assayed. Further experiments showed a similar rate of okadaic acid toxin production (pg cell^{-1} d^{-1}) for the 3 *Dinophysis* species under different T/S conditions. In contrast, a significant increment of gonyautoxin 4 content per cell was observed in *A. minutum* with decreasing S without significant effects associated with T. Our results highlight the response to environmental (T/S) stress of 3 species of *Dinophysis* and *A. minutum* with specific adaptations to thrive in different sub-habitats of the Galician Rías, an estuarine/coastal upwelling system in NW Spain.

KEY WORDS: *Dinophysis* · *Alexandrium* · Temperature and salinity stress · Diarrhetic shellfish poisoning · DSP · Paralytic shellfish poisoning · PSP · Harmful algal blooms

1. INTRODUCTION

Harmful algal blooms (HABs) in marine, brackish and freshwater systems are defined as any algal proliferation (regardless of cell density) that may cause massive fish kills, contaminate seafood with toxins and/or disrupt ecosystems in ways that humans perceive as harmful (GEOHAB 2001). Amongst a large variety of HABs, those of toxin-producing species which are transmitted through food webs via molluscan filter-feeders pose a threat to human health and represent the main natural risk for shellfish exploitations worldwide (Egmond et al. 1993, Granéli et al. 1999). Low biomass blooms of 3 toxigenic *Dinophysis* species, producers of diarrhetic shellfish toxins (DST) and/or pectenotoxins (PTX), are the main cause of

*Corresponding author: pilar.rial@ieo.csic.es
#Both authors contributed equally to this work

Publisher: Inter-Research · www.int-res.com

shellfish harvesting bans in the European Atlantic Arc (UK, Ireland, France, Spain and Portugal) (Belin et al. 2021, Bresnan et al. 2021). Additional harm may be caused by toxic HABs when toxins and other bioactive compounds are released or excreted (extracellular toxins) to the environment. In the field, relevant proportions of extracellular diarrhetic shellfish toxins (DST) and PTX2 have been found either in free form ('dissolved toxins' that pass through filters) or adsorbed onto organic aggregates in plankton samples even when *Dinophysis* cells were no longer present (MacKenzie et al. 2004, Pizarro et al. 2009). In culture experiments, PTX2 have been found to affect survival in early larval stages of fish (Rountos et al. 2019) and shellfish (Gaillard et al. 2021, Pease et al. 2022). Furthermore, Li et al. (2018) showed *in vitro* uptake of dissolved DSP toxins by mussels. These results suggest that extracellular toxins may represent an environmental threat, affecting recruitment of fish and shellfish and increasing toxin concentration in shellfish.

Alexandrium minutum produces paralytic shellfish toxins, and is the most frequent high-density bloom-forming species in Mediterranean coastal waters (Zingone et al. 2021). This species is associated with mild paralytic shellfish poisoning (PSP) events in Southern Europe and with water discolourations that cause social alarm in tourist resorts (Belin et al. 2021, Bresnan et al. 2021, Zingone et al. 2021). Harvesting is banned when toxins in shellfish exceed food safety regulatory limits (European Parliament and Council 2004, European Commission 2021). The impact of shellfish contamination with microalgal toxins is particularly high in western Iberia, where harvesting disruptions may last up to 9 mo in hot spots of DSP events (Blanco et al. 2005, Vale et al. 2008, Fernandes-Salvador et al. 2021). Understanding the mechanisms underlying the dynamics of HABs in a range of oceanographic regimes and how they are influenced by natural and anthropogenic factors is crucial to improve modelling and prediction of their occurrence (GEOHAB 2011).

Highly variable physical environments and nutrient regimes in estuaries and coastal waters drive the succession of phytoplankton assemblages (Margalef 1978, Smayda & Reynolds 2001, Glibert 2016). Regarding dinoflagellates, their observed diversity in upwelling systems is considered to reflect the mosaic of multiple and shifting sub-habitats present within these systems (Pitcher et al. 2010, Trainer et al. 2010). It is a challenge to understand how environmental processes select certain phytoplankton species that eventually burst into blooms (Carstensen et al. 2015). The mechanisms involved and the contribution of life-cycle transitions to bloom dynamics are usually poorly known (Wyatt 2014, Wyatt & Zingone 2014).

Temperature (T) and salinity (S) are important abiotic factors with direct effects on phytoplankton physiological processes (cell division, photosynthetic rates, life cycle transitions) (e.g. Figueroa et al. 2011) and often correlating with other algal growth and inhibition factors in complex ways. Indirect effects of T and S may add an important list of advantages (e.g. increased stability) for dinoflagellate species that overcome the physiological effects of increased T (Boyd et al. 2013). These include phenological changes (Guallar et al. 2017) and the extension of the phytoplankton growth season (Moore et al. 2015). Harmful dinoflagellate blooms are often related to T and S anomalies leading to marked density gradients and vertical stability (Díaz et al. 2016, 2021, Raine et al. 2018).

Likewise, heavy rainfall, ice melt and other freshwater inputs lead to a decline in S, the physiological effects of which can easily be masked by those related to stratification and runoff rich in humic and fulvic acids, plus additional nutrient input from human activities (Glibert 2017, Guallar et al. 2017).

Physiological experiments relating microalgal specific growth in response to these parameters frequently use wider ranges of T/S than those where field populations are found (Taylor 1987, Grzebyk et al. 2003).

In coastal upwelling regions, wind-forcing variations at interannual, seasonal and event scales influence the onset of the phytoplankton spring bloom and the annual succession of HABs (Pitcher et al. 2010, 2018). HABs in these systems are often produced by dinoflagellates and most of the habitat types where they may bloom, as defined by Smayda & Reynolds (2001), are encountered there. Changing physico-chemical conditions are the rule in these systems and organisms must adapt to short-term variations of abiotic factors and water column instability. In the Galician Rías, NW Spain, upwelling pulses from spring to autumn bring rapid (within hours) and marked changes in T and S which may drop considerably in the upper and middle reaches of the Rías after heavy rain in spring and autumn (Díaz et al. 2013, Velo-Suarez et al. 2014).

In the present study, the response to T and S stress in laboratory cultures of 3 species of *Dinophysis* (*D. acuminata*, *D. acuta* and *D. caudata*) and of *A. minutum* was studied using a combination of factorial design and mathematical growth modelling. These species, among the most frequent contributors to mussel toxicity in western Iberia, were selected because they exhibit marked differences in their life

cycle, physiology and spatial-temporal distribution (Bravo et al. 2010, Reguera et al. 2014). *Dinophysis* is a plastidic specialist non-constitutive mixotroph (pSNCM) sensu Mitra et al. (2016), i.e. an obligate mixotroph that steals plastids from a specific ciliate prey to photosynthesize (Garcia-Cuetos et al. 2010, Kim et al. 2012). Unlike *Alexandrium* species, no sexual cyst stages have been described in *Dinophysis*, but formation (by depauperating division, sensu von Stosch 1974) of small gamete-like cells has been observed in laboratory cultures and field populations of the 3 species under study. These small cells, which differ in size and shape from the mature vegetative cells, were formerly identified as separate species (*D. skagii*, *D. dens* and *D. diegensis* for the small cells of *D. acuminata*, *D. acuta* and *D. caudata*, respectively) (Reguera et al. 2012). Vegetative cells of *D. acuminata* are present throughout the year, whereas those of *D. acuta* occur only from late summer to early autumn and have a more neritic distribution. *D. caudata* often co-occurs with *D. acuta* in autumn (Pazos & Moroño 2008, Reguera et al. 2012, Velo-Suarez et al. 2014), and is the main *Dinophysis* species in tropical to warm-temperate waters (Larsen & Moestrup 1992). *D. caudata* is an important source of PTX in western Iberia (Fernández et al. 2008), the River Ebro Delta and in the Alboran Sea (Spanish Mediterranean coast) (Delgado et al. 2000, Fernández et al. 2008).

In contrast, the cyst-forming *A. minutum* is mainly autotrophic (Jeong et al. 2010) and grows in small embayments in the middle and outer reaches of the Rías. Its blooms, presumably self-seeded from the previous year's cysts in the sediments, develop in areas sheltered from the dynamic exchange of water between the Rías and the adjacent shelf. On the Galician coast, dense blooms (>10^7 cells l^{-1}) of *A. minutum* typically occur in spring and summer associated with stratified conditions induced by freshwater runoff (Blanco et al. 1985, Bravo et al. 2010, Nogueira et al. 2022).

The present study investigates the combined effects of T and S on the short-term (3–4 d) response (growth and toxin production) and recovery (>4 wk) in monoalgal cultures of 3 species of *Dinophysis* (*D. acuminata*, *D. acuta*, *D. caudata*) and of *A. minutum*. Since extracellular toxins in cultures of *D. acuta* are important (Nielsen et al. 2013), both intra- and extracellular fractions were analysed to quantify toxin excretion and rates of total toxin production under different situations of T/S stress.

The results identify species-specific windows of tolerance to these properties and permit parameterization of predictive models of their bloom development in the region.

2. MATERIALS AND METHODS

2.1. Cultures and culturing conditions

The dinoflagellate strains used in this work belong to the CCVIEO culture collection from the Oceanographic Centre of Vigo (IEO-CSIC) and were isolated from the Galician Rías Baixas, NW Spain. Details are listed in Table 1. The ciliate *Mesodinium rubrum* (AND-A071) and the cryptophyte *Teleaulax amphioxeia* (AND-A070) used for mixotrophic cultures of *Dinophysis* were isolated from water samples collected off Huelva (SW Iberian Peninsula). Cultures were grown in diluted (1/20) $L1_{-Si}$ medium for *D. acuminata* and *D. caudata*, $L1_{-Si}$ medium for *Alexandrium minutum* (Guillard & Hargraves 1993) and modified K medium (Keller et al. 1987), with no silicate or nitrate added for *D. acuta*. They were all prepared with filtered (0.22 µm pore size) and autoclaved seawater, with pH 8.00 ± 0.02 (SE) and S of 32. Growth T was 19°C for *D. acuminata*, *D. caudata* and *A. minutum*, and 15°C for *D. acuta*. The light regime was a 12 h light:12 h dark photoperiod, with 150 µmol photons m^2 s^{-1} irradiance for *D. acuminata* and *D. caudata*, 75 for *D. acuta* and 90 µmol photons m^2 s^{-1}

Table 1. The *Dinophysis* spp. and *Alexandrium minutum* strains used in this study, and temperature (T) and salinity (S) ranges (CTD casts, 0–15 m in Bueu and Toralla; 0–34 m in E1VI) observed at the stations

Species (strain)	Collection date	Collection site	T (°C)	S
D. acuminata (VGO1411)	Jul 2019	Toralla (42° 19.71′ N, 8° 52.32′ W)	11.87–17.34[a]	29.81–35.73[a]
D. acuta (VGO1065)	Oct 2010	Bueu (42° 21.40′ N, 8° 46.42′ W)	12.55–20.00[a]	31.40–35.91[a]
D. caudata (VGO1396)	Jul 2016	E1VI (42° 13.3′ N, 8° 51.0′ W)	11.87–17.34[b]	29.81–35.77[b]
A. minutum (VGO1439)	Jul 2018	A Laxe (42° 14.04′ N, 8° 43.72′ W)	12.85–17.85[c]	29.81–35.73[a]

[a]INTECMAR; [b]RADIALES-VIGO (https://www.seriestemporales-ieo.net); [c]COPERNICUS SERVICES (www.copernicus.eu)

for *A. minutum*. Irradiance was delivered by Osram LED 30 W-cold light, 6400 K tubes. Mixotrophic cultures of *Dinophysis* spp. were periodically fed (1:10 predator:prey ratio) the ciliate *M. rubrum* (AND-A071) and the cryptophyte *T. amphioxeia* (AND-A070). Cultures were non-axenic.

2.2. Expt 1: effects of T and S stress on growth

Culture conditions used for the experiment were similar to those for culture maintenance but with lower irradiance (45 µmol photons m^2 s^{-1} of photosynthetically active radiation [PAR]) and a 12 h light:12 h dark cycle. A gradient matrix with 5 T (12.5, 14.4, 19, 23.6 and 25.5°C) and 5 S (5, 9.7, 21, 32.3 and 37) values was built to test the combined effect of both factors on the growth of prey-deprived cultures of *D. acuminata* (VGO1411), *D. acuta* (VGO1065) and *D. caudata* (VGO1396) and auxotrophic cultures of *A. minutum* (VGO1439). These treatments were chosen taking into account the range of T (11.12–20.29°C) and S (30.46–35.94) values observed in CTD casts (top 10 m) from a representative station in Ría de Vigo, between 1994 and 2020, in the framework of the IEO monitoring project Radiales (https://www.seriestemporales-ieo.net/) (see Fig. S1 in the Supplement at www.int-res.com/articles/suppl/a089p001_supp.pdf).

Cultures were grown in 3 chambers at 15, 19 and 25.5°C and the 5 experimental conditions required (12.5, 14.4, 19, 23.6 and 25.5°C) were set as follows: 19 and 25.5°C were incubated in the corresponding chambers (actual T ranges of 19.0 ± 0.5 and 24.6 ± 1.0°C, respectively). In turn, 12.5, 14.4 and 23.6°C required the use of 3 Aqua Medic Titan 1600 cooling units (AB Aqua Medic; accuracy 0.1°C).

The experimental range of T and S exceeded that in the Rías (Vigo and Pontevedra) where the strains were collected (Table 1).

Well-fed cultures of each *Dinophysis* species and a dense culture in the exponential phase of *A. minutum* were divided into 13 aliquots (Fig. S2). An aliquot for each *Dinophysis* species was previously subjected to reverse filtration through a nylon sieve (mesh size, 20 µm) to remove any remaining cells of *M. rubrum* and cryptophytes; filtered *Dinophysis* spp. cells were resuspended in fresh culture medium with no prey added. All the experiments were carried out under the same irradiance and T/S combinations, in 200 ml volume, at initial concentrations of 150 cells ml^{-1} of *Dinophysis* spp. and 2×10^3 cells ml^{-1} of *A. minutum*.

Samples to estimate cell densities were taken every 2–3 d, fixed with acidic Lugol's solution (0.5%) and 2 aliquots of each sample counted in 1 ml Sedgwick-Rafter (Pyser Optics) counting chambers with a Zeiss Invertoscop D microscope at 100×. The whole surface of the chamber was scanned and counted.

2.3. Expt 2: effects of T/S on toxin production and accumulation

Based on results from Expt 1, two treatments were chosen with the same T (12.5°C) and 2 values of S (21 and 35.5) for *Dinophysis* spp., to estimate toxin production rates (pg $cell^{-1}$ d^{-1}). Estimates of intracellular (particulate) toxins, the parameter usually measured in field populations, were expressed as toxin content per cell (toxin quota, pg $cell^{-1}$) and as toxin per unit of biovolume (fg $µm^{-3}$) in *Dinophysis* spp. and as bioarea (fg $µm^{-2}$) in *A. minutum*. Toxins per unit of biovolume is a normalized way to express toxin content which allows us to distinguish whether increased toxin per cell (quota) is due to an imbalance between cellular division (negative) and toxin production (positive).

Well-fed cultures of *D. acuta* and *D. acuminata* were divided into 6 aliquots, each subjected to reverse filtration as in Expt 1 and the filtered cells resuspended (×3) in fresh medium and further divided into 2 T/S treatments (12.5°C/21 and 12.5°C/35.5), with the same inoculum density and irradiance as in Expt 1. Cultures were grown at 12.5°C with Aqua Medic Titan 1600 cooling units (AB Aqua Medic; accuracy 0.1°C). Cultures were sampled every 2–3 d for 10 d. Two aliquots were taken from each flask: 5 ml for toxin extraction and 1.5 ml for cell counting and measurements.

For *A. minutum*, growth conditions were identical to Expt 1, but only 2 combinations of T (15 and 25°C) and S (10 and 30) were chosen. Cultures were grown in chambers at 15 and 25°C (Equitec EGCHS 755/3; accuracy 0.1°C). Each treatment had 3 replicates with 1 sub-replicate (so that the same experimental setup could be followed without compromising the culture volume during sampling). Samples were taken once a week for 3 wk: 1.1 ml for cell counting (following the procedure described in Section 2.2) and 40 ml for cell measurements and toxin extractions.

2.4. Cell measurements

2.4.1. *Dinophysis* spp.

Measurements of at least 30 vegetative and 15 small cells of *Dinophysis* spp. per sample were made with

a Leica microscope coupled to an Axio CamHR3 camera system using ZEN 2012 software. Longitudinal axis (L), and breadth (G) and dorso-ventral depth (H) of the large hypothecal plates were measured according to Balech (2002) and their mean value ($\bar{L}$, $\bar{H}$, $\bar{G}$) in each sample used to estimate total biovolume contributed by vegetative and small cells per ml of culture. Cell biovolumes (V) of *Dinophysis* spp. were calculated according to Sun & Liu (2003):

$$V = \frac{\pi}{6} \times \bar{L} \times \bar{H} \times \bar{G} \quad (1)$$

2.4.2. *Alexandrium minutum*

The bioarea of *A. minutum* cells was estimated using imaging flow cytometry (IFC). Each 20 ml sample was fixed with 20% formaldehyde for 24–48 h. Samples were then centrifuged at 5000 × *g* for 5 min at 10°C, the supernatant discarded and the same step repeated; the final pellet was resuspended in 1.5 ml of cold methanol and stored at 4°C for at least 12 h to facilitate chlorophyll extraction. The sample extracts were centrifuged at 5000 × *g* for 5 min at 10°C, the cells washed in phosphate-buffered saline (PBS) solution (pH 7, Sigma-Aldrich) and the pellet resuspended in staining solution (300 µl propidium iodide [Sigma-Aldrich] and 30 µl RNase A [Sigma-Aldrich] ml^{-1} in PBS) for at least 2 h in darkness before analysis. A Flow Sight image flow cytometer (Amnis) equipped with 2 lasers, emitting at 488 and 405 nm, was used. Before starting the analysis, samples were centrifuged at 5000 × *g* for 5 min and 10°C and 250 µl of PBS added to remove the iodide. The samples were run at low speed and data acquired until 3000–10 000 events were recorded. Cellular surface (bioarea) was measured using the Ideas 6.0 (Amnis) software.

2.5. Extraction and analysis of toxins

2.5.1. *Dinophysis* spp.

Two different fractions were collected for toxin analysis in *Dinophysis* spp. cultures: particulate (intracellular) and extracellular (dissolved) toxins. Total toxin content per unit of culture volume was estimated as the sum of particulate and extracellular toxins.

Samples for analysis of particulate (intracellular) toxins in *D. acuminata* and *D. acuta* cultures were filtered through GF/C filters (Whatman); the filter with the filtered cells was placed in an Eppendorf tube with 750 µl MeOH, sonicated for 30 s at 50 W and centrifuged at 10 000 × *g* and 10°C for 10 min (Sigma 3-16K2 Sartorius centrifuge). Supernatants were collected in clean Eppendorf tubes. The extraction procedure was repeated, the 2 supernatants combined and the final volume adjusted to 1.5 ml. The filtrate was collected in a 10 ml tube for further processing.

To identify and quantify free and esterified okadaic acid (OA) and dinophysistoxins (DTX), the methanolic extracts were subjected to alkaline hydrolysis before the liquid chromatography–mass spectrometry (LC/MS) analysis by adding 125 µl of 2.5 M NaOH. The previous mixture was homogenized with a vortex for 30 s and heated in a water bath at 76°C for 40 min. After cooling, the extract was neutralized with 125 µl of 2.5 M HCl, homogenized again with vortex for 30 s, filtered through a dry methanol-compatible 0.2 µm pore size syringe filter and a 5 µl aliquot injected onto the LC column. Chromatographic separation was performed on a Gemini NX-C18 (100 × 2 mm, 3 µm) column following the liquid chromatography/high-resolution mass spectrometry (LC-HRMS) method detailed in Rodríguez et al. (2018). Limit of detection (LOD) and limit of quantification (LOQ) of the LC-MS system were: for OA and DTX2, LOD = 2 ng ml^{-1} (10 pg on column) and LOQ = 5 ng ml^{-1} (25 pg on column); for PTX2, LOD = 0.2 ng ml^{-1} (1 pg on column) and LOQ = 0.6 ng ml^{-1} (3 pg on column).

For extracellular toxins, 5 ml of culture filtrates were passed through Sep-Pak vac tC18 3cc cartridges previously activated with 3 ml of 100% MeOH and washed with 3 ml of Milli-Q water. Next, the cartridge samples were washed with 4 ml of 20% MeOH, eluted with 4 ml of 100% MeOH and the eluate dried at 40°C on a Speed Vac (Savant Instruments) under reduced pressure, re-suspended in 500 µl of MeOH, and subjected to hydrolysis by adding 62.5 µl of 2.5 M NaOH to 500 ml of methanolic extract. Alkaline hydrolysis was carried out as described above. The extract obtained was filtered through 0.22 µm filters (13 mm hydrophilic PTFE syringe filter, Filter-Lab) prior to injection into the LC-MS system following the same LC-HRMS method as with particulate toxins.

2.5.2. *Alexandrium minutum*

Samples (40 ml) from *A. minutum* cultures were filtered through glass fibre filters (GF/C 25 mm diameter; Whatman). Each filter was placed in an

Eppendorf tube, 750 µl 0.05 M acetic acid added and the content of each tube sonicated for 1 min at 50 W and kept at −20°C until analysis. For toxin extraction, samples were thawed and centrifuged at approx. 18 000 × *g* at 10°C for 10 min (Sigma 3-16KL Sartorius centrifuge), the supernatants collected in clean Eppendorf tubes and the extraction steps repeated. Both supernatants were combined (final volume 1500 µl) and then filtered through 0.22 µm PTFE syringe filters prior to high-performance liquid chromatography (HPLC) analyses.

Determination of paralytic shellfish toxins (PSTs) was carried out according to the liquid chromatography post-column oxidation followed by fluorescence detection (LC-PCOX-FLD) method of Rourke et al. (2008) with some modifications as described in Rodríguez et al. (2016). The ultra performance liquid chromatography (UPLC) equipment, post-column reaction system and reagents, mobile phases, gradient conditions and FLD detector wavelengths employed were as in Rodríguez et al. (2016). Chromatographic separation was performed with a Waters XBridge® Shield RP, 4.6 × 150 mm, 3.5 µm column. Certified reference PST standards were purchased from the National Research Council Canada (NRC-CRMs).

In a recent study, Ben-Gigirey et al. (2020) showed that the toxin profile of a clonal culture of *A. minutum* VGO1439 was dominated by gonyautoxin 4 (GTX4) with trace amounts of GTX3 and GTX2. Therefore, only changes in GTX4 production under different treatments were analysed in the present study. This simplified the chromatographic method to a flow of 95% solvent A and 5% solvent B at 1 ml min^{-1} and run time was reduced to 20 min.

2.6. Growth and toxin production rates

Specific growth rates (µ, d^{-1}) were estimated following Guillard (1973):

$$\mu = \frac{\ln N_2 - \ln N_1}{t_2 - t_1} \quad (2)$$

where N_1 and N_2 are cell densities (cells ml^{-1}) at time t_1 and t_2 (days). In the case of *Dinophysis* spp. cultures, 2 values of µ were estimated for each treatment and culture: an average µ (μ_{0-10}) from Days 0 to 10, and μ_{max}, for the time interval within the growth curve when the maximal slope was observed.

R_{tox}, the specific toxin production rate (particulate + dissolved), expressed as pg of toxin $cell^{-1}$ d^{-1}, was calculated as:

$$R_{tox} = \frac{T_2 - T_1}{\bar{N}(t_2 - t_1)} \quad (3)$$

where T_1 and T_2 are the total toxin content per ml of culture (particulate + dissolved) from 2 samples collected on t_1 and t_2, and N is the ln average of the cell concentration per ml calculated as:

$$\bar{N} = \frac{N_2 - N_1}{\ln(N_2 / N_1)} \quad (4)$$

The toxin content (*Tox*) or accumulation per unit of biovolume (*Biovol*, μm^{-3}) was estimated by dividing the particulate toxin (T_p) content by the cell biovolume per ml.

$$Tox = \frac{T_p}{Biovol} \quad (5)$$

2.7. Statistical analysis

2.7.1. Response surface methodology (RSM)

The joint effects of 2 independent variables, T and S, on the growth of *D. acuminata*, *D. acuta*, *D. caudata* and *A. minutum* were studied with a second-order rotatable design (Box-Behnken design) (Box et al. 2005). This design is based on the combination of 5 levels of the 2 variables under study (in coded values): −1.41, −1, 0, 1 and 1.41 to generate 8 running treatments and 5 replicates in the centre of the experimental domain (0, 0) (Table 2). This design assures a full statistical analysis with reduced risk of type I and type II statistical errors (Fig. S3). The evaluated response was the normalized growth, N/N_0, where N is cell density at a selected point in the growth curve and N_0 is cell density at the beginning of the experiment (the inoculum). Experimental T (in the range of 12.5–25.5°C) and S (in the range of 5–37) used and procedures for codification-decodification of the vari-

Table 2. Temperature (T) and salinity (S) conditions used in the factorial design experiment

T (°C)	T codified	S	S codified	No. of replicates
14.4	−1	9.7	−1	1
14.4	−1	32.3	1	1
12.5	−1.41	21.0	0	1
19.0	0	5.0	−1.41	1
19.0	0	37.0	1.41	1
19.0	0	21.0	0	5
23.6	1	9.7	−1	1
23.6	1	32.3	1	1
25.5	1.41	21.0	0	1

ables are summarized in Table S1. Codification of the variables is essential to avoid the high statistical weight that the actual values may produce in the statistical analysis when there are numerical differences between the natural variables (Akhnazarova & Kafarov 1982, Box et al. 2005). This problem is solved by encoding the 2 variables, and thus the coefficients of the empirical equation are not distorted by the natural values of the variables.

Orthogonal least-square calculations with the factorial design data were used to obtain the empirical equations describing the mathematical relationship between N/N_0 and the independent variables T and S following the equation below:

$$Y = b_0 + \sum_{i=1}^{n} b_i X_i + \sum_{\substack{i=1 \\ j>i}}^{n-1} \sum_{j=2}^{n} b_{ij} X_i X_j + \sum_{i=1}^{n} b_{ii} X_i^2 \qquad (6)$$

where Y represents the normalized growth (N/N_0); b_0 is the constant coefficient, b_i is the coefficient of linear effect, b_{ij} is the coefficient of interaction effect, b_{ii} the coefficients of squared effect, n is the number of variables and X_j and X_i define the independent variables (T and S). A Student t-test ($\alpha = 0.05$) was used to determine the statistical significance of the coefficients. The goodness of fit was established as the determination coefficient (R^2) and the adjusted determination coefficient (R^2_{adj}). In addition, the model consistency was validated by the Fisher F-test ($\alpha = 0.05$) using the following mean squares ratios (Table S2).

F^{num}_{den} are the theoretical values to $\alpha = 0.05$ with the corresponding degrees of freedom for the numerator (num) and denominator (den). The equation is acceptable when *F1* and *F2* are validated. *F3* and *F4* were additionally calculated to improve the degree of robustness and consistency of the empirical equations obtained. Response surfaces from second-order factorial designs and statistical analysis were calculated by means of Statistica v. 8.0 software (StatSoft).

2.7.2. Other analyses

The normalized growth, defined as the N/N_0 ratio, was used in all *Dinophysis* spp. growth calculations. Statistical analyses, performed with RStudio v. 3.6.1 software, included: the Shapiro-Wilk normality test to check the 'normality hypotheses', Bartlett's K-squared test for variance homogeneity and the Durbin-Watson test for the independence of the variable. When these 3 conditions were met, a 1-way ANOVA was applied; otherwise the non-parametric Kruskal-Wallis test was used. To compare only 2 variables, the Shapiro-Wilk and Wilcoxon test were applied. Differences were considered statistically significant when $\rho < 0.05$, for a significance level of $\alpha = 0.05$.

3. RESULTS

Dinophysis species and *Alexandrium minutum* showed differing responses to T and S stress in growth rates, toxin dynamics and morphology.

3.1. Effects on growth rates

3.1.1. *Dinophysis* spp. growth

Relevant differences in specific growth rates were observed between the 3 species of *Dinophysis* during the first 10 d of T/S stress. None of the 3 species survived at the lowest S levels (5 and 9.7) (Fig. 1, Tables 3 & S3). At S of 21, *D. acuminata* (Fig. 1A–C) and *D. acuta* (Fig. 1D–F) did not grow when maintained at 25.5°C, but positive growth was observed if combined with a lower T (12.5 and 19°C). *D. caudata* (Fig. 1G–I) showed positive growth under the 3 T/S treatments (14.4°C/32.3, 19°C/37, 23.6°C/32.3) with S > 32 and survived (with no growth) for 20 d at T/S 19°C/21. In summary, *D. acuminata* and *D. acuta* showed positive growth with 5 of the 9 T/S combinations assayed; *D. caudata* grew under 3 of them and tolerated a fourth one. Growth rates of *D. acuminata*, *D. caudata* and *D. acuta* in the first 10 d were very low ($\mu < 0.1$ d^{-1}).

D. acuminata showed similar growth rates in 2 of the treatments, with highest values at T/S 12.5°C/21. Maximal growth rates (μ_{max} = 0.07 d^{-1}) were observed with 19°C/37, between Days 14 and 19.

D. acuta showed similar low growth rates and values ($\mu \approx 0.04$) in 3 of the T/S treatments: 23.6°C/32.3, 14.4°C/32.3 and 19°C/21. As with *D. acuminata*, maximal growth rate (μ_{max} = 0.11 d^{-1}) was observed at 19°C/37, between Days 12 and 17.

D. caudata showed its highest growth rate (μ = 0.05 d^{-1}) in the first 10 d at T/S 19°C/37 and 23.6°C/32.3, and maximal growth (μ_{max} = 0.09 d^{-1}) with 23.6°C/32.3 between Days 25 and 34 (Table 3).

Cell densities (yield) attained in each treatment are listed in Table S3. Contamination with a tiny flagellate was observed in *D. acuta* cultures, which were prepared with full-strength K medium.

Statistical analyses (significance, Kruskal-Wallis test) of the response of each species to different treatments showed that both T and S had the same in-

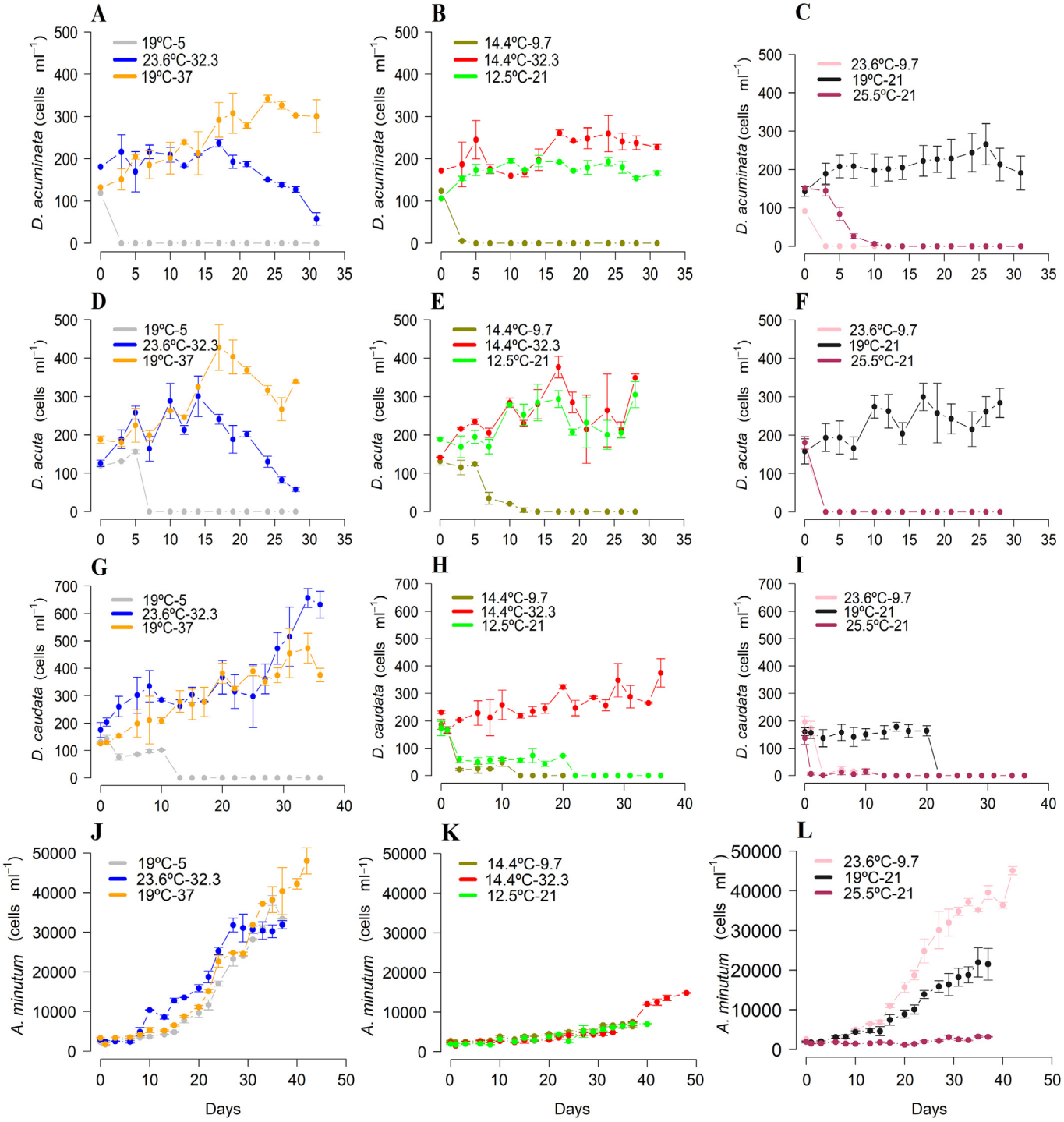

Fig. 1. Growth curves of (A–I) *Dinophysis* species (A–C: *D. acuminata*, D–F: *D. acuta*, G–I: *D. caudata*) and (J–L) *Alexandrium minutum* under 9 different combinations of temperature (T) (12.5, 14.4, 19, 23.6 and 25.5°C) and salinity (S) (5, 9.7, 21, 32.3 and 37). Error bars represent the standard deviation (SD) (not drawn when the error bar was smaller than the symbol)

fluence on *D. acuminata* ($\rho = 2.2 \times 10^{-16}$); in the case of *D. acuta* and *D. caudata*, S ($\rho = 2.2 \times 10^{-16}$) had a stronger influence than T ($\rho = 1.06 \times 10^{-12}$ and 2.98×10^{-8}, respectively) and this difference was more marked in the case of *D. caudata*.

3.1.2. *Alexandrium minutum* growth

Growth rates were calculated during the exponential phase, which implied using different days depending on the treatment (Table 3). The highest rate

Table 3. Average (μ_{0-10}: first 10 d) and maximal (μ_{max}) growth rate estimates for *Dinophysis* spp. and *Alexandrium minutum* cultures with different temperature (°C) and salinity (T/S) treatments (blank cells correspond to culture conditions where cells did not survive)

T/S	μ_{0-10} (d^{-1})				μ_{max} (d^{-1})			
	D. acuminata	*D. acuta*	*D. caudata*	*A. minutum*	*D. acuminata*	*D. acuta*	*D. caudata*	*A. minutum*
14.4/9.7	–	–	–	0.034	–	–	–	μ_{15-31} = 0.025
14.4/32.3	–0.007	0.041	0.012	0.015	μ_{10-17} = 0.070	μ_{12-17} = 0.098	μ_{22-29} = 0.049	μ_{20-40} = 0.070
23.6/9.7	–	–	–	0.067	–	–	–	μ_{15-33} = 0.093
23.6/32.3	0.015	0.044	0.050	0.132	μ_{12-17} = 0.051	μ_{7-14} = 0.087	μ_{25-34} = 0.088	μ_{13-27} = 0.093
19/5	–	–	–	0.044	–	–	–	μ_{15-35} = 0.094
19/37	0.042	0.023	0.053	0.048	μ_{14-19} = 0.074	μ_{12-17} = 0.111	μ_{25-34} = 0.022	μ_{13-42} = 0.077
12.5/21	0.061	0.024	–	0.047	μ_{0-10} = 0.061	μ_{7-14} = 0.074	–	μ_{13-37} = 0.044
25.5/21	–	–	–	–0.031	–	–	–	μ_{1-29} = 0.027
19/21	0.033	0.043	–0.005	0.084	μ_{17-26} = 0.020	μ_{7-17} = 0.059	–	μ_{15-35} = 0.078

(μ = 0.09 d^{-1}) was observed at T/S 19°C/5 followed by 23.6°C/9.7 (μ = 0.09 d^{-1}). Lowest rates were found at 14.4°C/9.7 and 25.5°C/21 (μ = 0.03 d^{-1} in both cases), and the optimal T window for cell yield was between 19.0 and 23.6°C (Table 3). S was not relevant for *A. minutum* growth. A positive relationship between growth and T was observed throughout the experiment, except at 25.5°C (Fig. 1J–L). In cultures at 23.6°C, cell densities showed an immediate exponential increase at all values of S. With lower T (19°C), final cell yields were 50 % lower. With T above and below the optimal window, growth rates were almost zero (Table 3).

3.2. Changes in cell size

3.2.1. *Dinophysis* spp. size and small cell formation

In cultures of *D. acuminata*, only a few small cells were detected. Formation of small (*D. dens*-like) cells (L = 53.9 ± 0.6 µm, H = 30.39 ± 0.8 µm) in cultures of *D. acuta* was noticeable (0.7–23 %) in the stationary and/or declining phases of the cultures with higher growth rates. The highest frequency of small cells (23 %) was found in the stationary phase (Day 24) with T/S 23.6°C/32.3, followed by 19°C/21 and 19°C/37. Aberrant cells, i.e. specimens with a rudimentary development of the cingular and sulcal lists and lacking mobility, were observed in the same treatment (23.6°C/32.3), in particular during the stationary phase (1.9 % on Day 5, 18.6 % on Day 21). Frequencies of aberrant cells (0.2–1.9 %) observed in the other treatments during late exponential and stationary phases were very low. Small cells of *D. caudata* (L = 56 ± 2 µm, H = 24.89 ± 2 µm) were found in different proportions (0.4–10.7 %) and phases in all the treatments tolerated by this species. Maximal frequency was found with the 19°C/37 treatment during the exponential phase. Aberrant cells were not detected in cultures of this species (Table 4).

3.2.2. Changes in cell size in *Alexandrium minutum*

No significant changes in the bioarea of *A. minutum* were observed in samples collected at the end of the experiment (n ≥ 3000 cells, 1 exception with n = 450 cells). The highest bioarea (556.12 μm^2) was ob-

Table 4. Small and aberrant cells observed in *Dinophysis acuta* and *D. caudata* with different temperature (°C) and salinity (T/S) treatments. Init. day: day that small or aberrant cells were first observed; Max. day: day that the % of small or aberrant cells was highest; last 2 empty rows for *D. caudata* correspond to cultures that did not survive under that T/S treatment

T/S	*D. acuta*								*D. caudata*			
	Small cells				Aberrant cells				Small cells			
	Init. day	%	Max. day	%	Init. day	%	Max. day	%	Init. day	%	Max. day	%
19/37	5	0.8	24	9	19	0.2	21	0.52	3	1	15	10.7
23.6/32.3	5	0.75	24	23	5	1.9	21	18.6	3	0.45	34	2.75
14.4/32.3	7	2.3	10	4.8	19	0.3	28	1.3	8	3.41	8	3.41
12.5/21	10	1.8	26	11.6	14	0.7	21	1.6				
19/21	7	1.7	24	14	10	0.7	21	2.5				

Table 5. Mean size and range (minimum–maximum) of *Alexandrium minutum* cell measurements by the final phase of the experiment. T: temperature (°C); S: salinity

T/S	No. of cells	Mean size (µm^2)	Minimum size (µm^2)	Maximum size (µm^2)
15/10	3119	509.89	163	924
15/30	3074	552.66	225	942
25/10	5138	556.12	179	931
25/30	4097	516.14	169	907

served in cells grown at T/S 25°C/10 followed by those at 15°C/30 (552.66 µm^2; Table 5).

3.3. Response-surface analysis (RSA)

The combined effect of T and S on normalized growth (N/N_0) (experimental data and predicted growth surfaces) evaluated with RSA at selected times of culture are depicted in Figs. 2 & 3. Numeri-

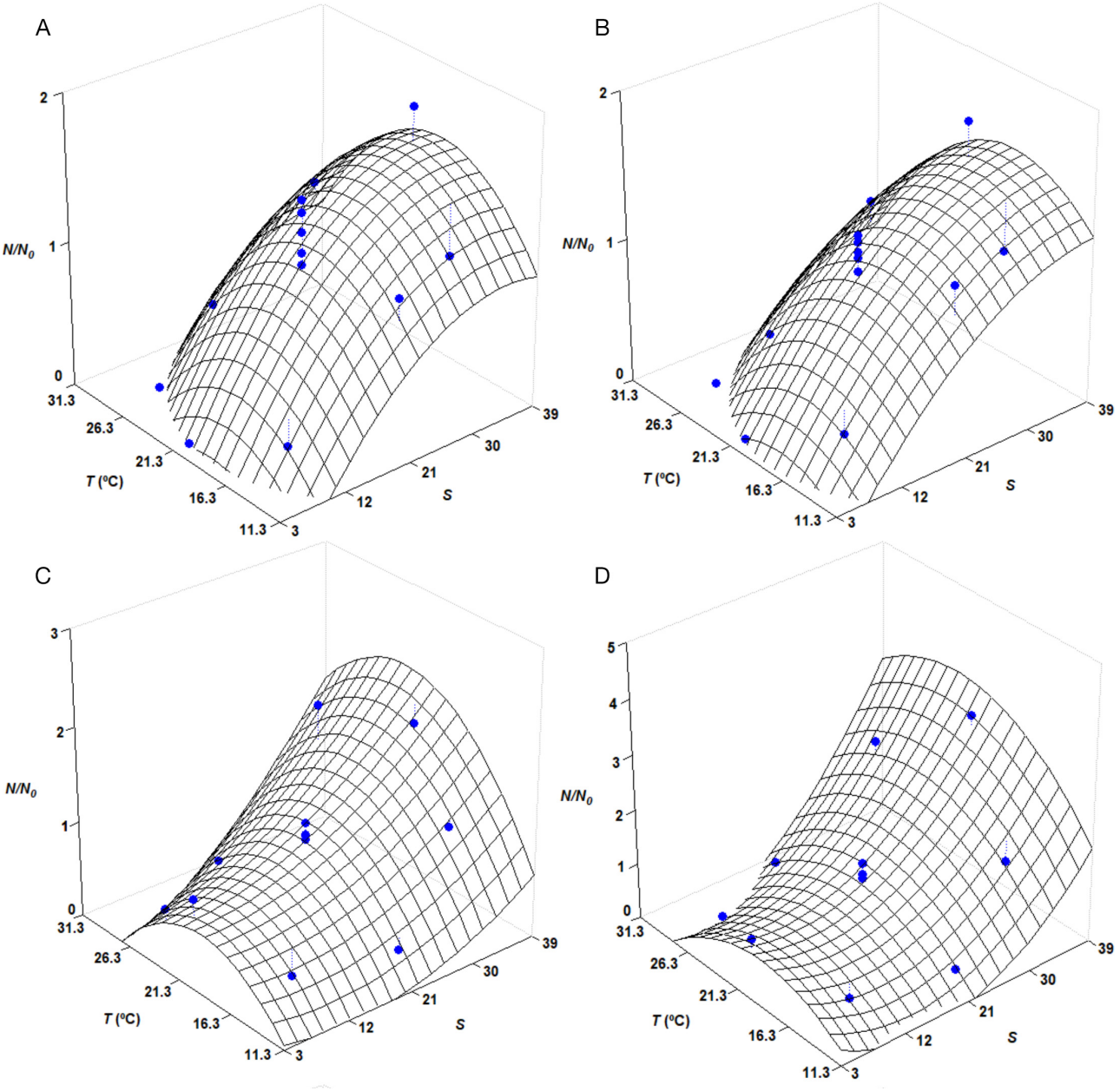

Fig. 2. (Above and following page.) Experimental data (blue dots) and predicted response surfaces describing the combined effect of temperature (T) and salinity (S) on the (A,C,E) exponential and (B,D,F) stationary growth phase of *Dinophysis* species. The *y*-axes are represented as normalized growths (N/N_0). (A) *D. acuminata* (Day 10); (B) *D. acuminata* (Day 17); (C) *D. caudata* (Day 10); (D) *D. caudata* (Day 20); (E) *D. acuta* (Day 12); (F) *D. acuta* (Day 28)

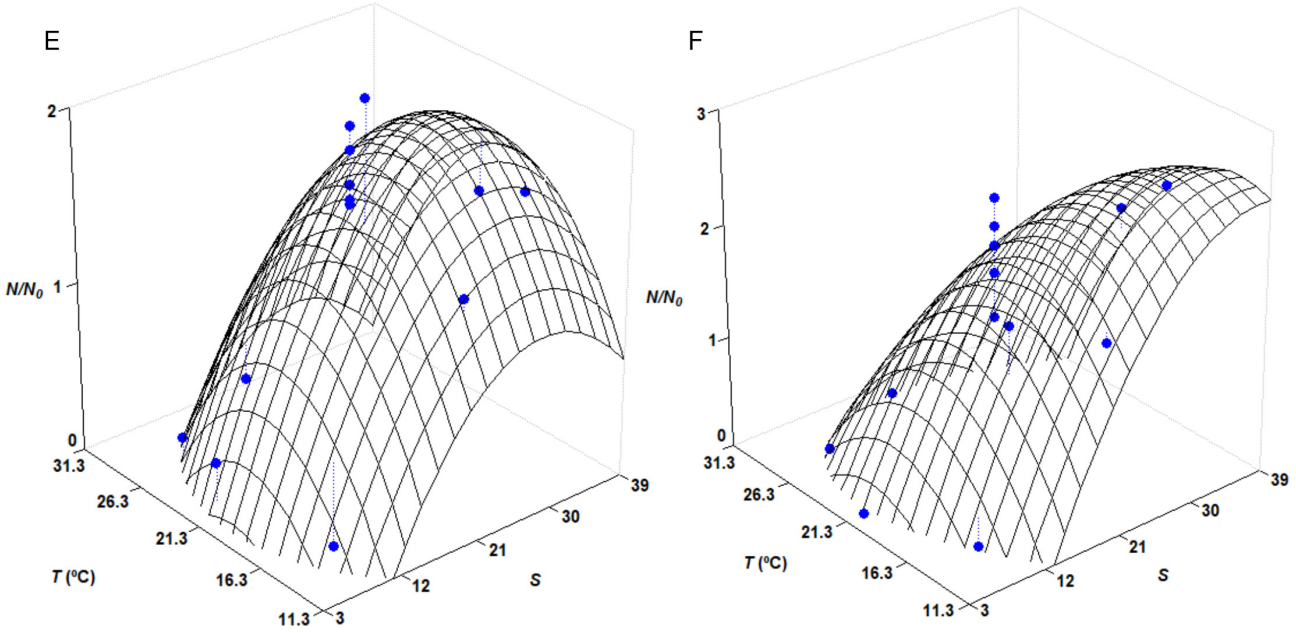

Fig. 2. (continued)

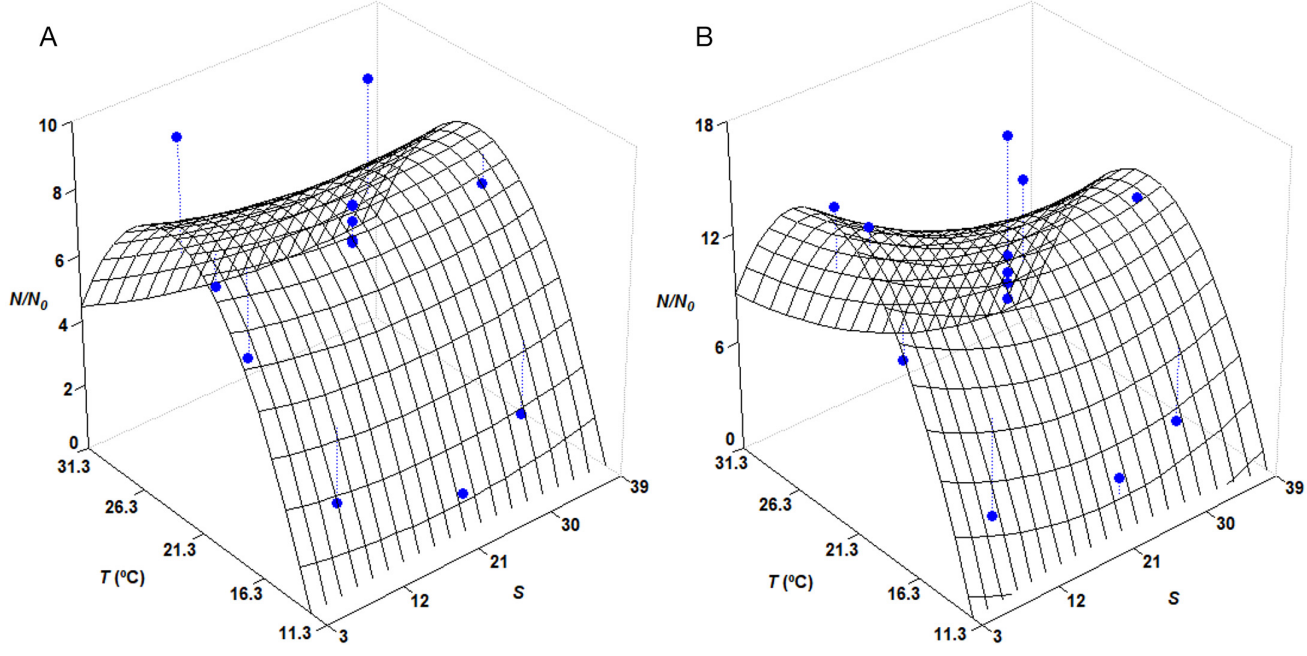

Fig. 3. Experimental data (blue dots) and predicted response surfaces describing the simultaneous effect of temperature (T) and salinity (S) on the (A) exponential (Day 24) and (B) stationary (Day 37) growth phase of *Alexandrium minutum*. The *y*-axes are represented as normalized growths (N/N_0)

cal results, including polynomial equations, statistical analysis and optimal values of both variables for the 3 species of *Dinophysis* and for *A. minutum*, are summarized in Tables 6 & 7. Results for *Dinophysis* spp. showed that negative quadratic coefficients for T were statistically significant in all cultures (Student *t*-test for $\alpha = 0.05$). Linear parameters for T were significant in only 50 % of the cases. Linear coefficients for S were positive in most cases (increasing growth at increasing T and S). Second-order terms revealed interspecific differences (Fig. 2). A remarkably high goodness of fit of the empirical equations (agreement

Table 6. Summary of polynomial equations describing the joint influence of salinity (S) and temperature (T) in the growth (as N/N_0) of different strains of *Dinophysis* at 2 different times of the growth curve. See Section 2.7 for definitions of parameters. Optimal values for both independent variables (S_{opt}, T_{opt}) to reach the predicted growth maxima (Y_{max}) were also calculated. Sig.: significant; NSig.: non-significant

Parameter	*D. acuminata* 10 d	*D. acuminata* 17 d	*D. caudata* 10 d	*D. caudata* 20 d	*D. acuta* 12 d	*D. acuta* 28 d
b_0 (intercept)	1.13 ± 0.23	0.98 ± 0.12	1.01 ± 0.10	1.03 ± 0.14	1.69 ± 0.24	1.86 ± 0.50
b_1 (S)	0.53 ± 0.18	0.49 ± 0.10	0.47 ± 0.08	0.80 ± 0.11	−0.57 ± 0.19	0.69 ± 0.30
b_2 (T)	NSig.	−0.25 ± 0.10	NSig.	NSig.	−0.20 ± 0.19	−0.54 ± 0.30
b_{12} (S × T)	NSig.	NSig.	0.17 ± 0.11	0.22 ± 0.16	NSig.	NSig.
b_{11} (S^2)	NSig.	−0.13 ± 0.10	0.13 ± 0.08	0.41 ± 0.12	−0.42 ± 0.20	−0.51 ± 0.40
b_{22} (T^2)	−0.29 ± 0.20	−0.24 ± 0.10	−0.38 ± 0.08	−0.42 ± 0.12	−0.46 ± 0.20	−0.56 ± 0.40
R^2	0.746	0.905	0.927	0.975	0.841	0.847
R^2_{adj}	0.696	0.857	0.890	0.962	0.762	0.771
F1	14.71	18.97	25.3	76.85	10.61	11.08
	$[F^2_{10} = 4.10] \Rightarrow$ Sig.	$[F^4_8 = 3.84] \Rightarrow$ Sig.	$[F^4_8 = 3.84] \Rightarrow$ Sig.	$[F^4_8 = 3.84] \Rightarrow$ Sig.	$[F^4_8 = 3.84] \Rightarrow$ Sig.	$[F^4_8 = 3.84] \Rightarrow$ Sig.
F2	0.324	0.546	0.535	0.510	0.581	0.557
	$[F^8_2 = 19.37] \Rightarrow$ Sig.	$[F^8_4 = 6.04] \Rightarrow$ Sig.	$[F^8_4 = 6.04] \Rightarrow$ Sig.	$[F^8_4 = 6.04] \Rightarrow$ Sig.	$[F^8_4 = 6.04] \Rightarrow$ Sig.	$[F^8_4 = 6.04] \Rightarrow$ Sig.
F3	3.11	3.94	4.87	2.06	3.47	1.35
	$[F^{10}_4 = 5.96] \Rightarrow$ Sig.	$[F^8_4 = 6.04] \Rightarrow$ Sig.	$[F^8_4 = 6.04] \Rightarrow$ Sig.	$[F^8_4 = 6.04] \Rightarrow$ Sig.	$[F^8_4 = 6.04] \Rightarrow$ Sig.	$[F^8_4 = 6.04] \Rightarrow$ Sig.
F4	4.51	6.89	8.74	3.11	5.94	1.69
	$[F^6_4 = 6.16] \Rightarrow$ Sig.	$[F^4_4 = 6.39] \Rightarrow$ NSig.	$[F^4_4 = 6.39] \Rightarrow$ NSig.	$[F^4_4 = 6.39] \Rightarrow$ Sig.	$[F^4_4 = 6.39] \Rightarrow$ Sig.	$[F^4_4 = 6.39] \Rightarrow$ Sig.
S_{opt}	> 37	> 37	> 37	> 37	28.8	28.7
T_{opt} (°C)	19.0	16.7	20.6	20.8	18.0	16.8
Y_{max} (as N/N_0)	1.93	1.48	2.04	3.22	1.91	2.23

Table 7. As in Table 6, but for *Alexandrium minutum*

Parameter	*A. minutum* 24 d	*A. minutum* 37 d
b_0 (intercept)	7.37 ± 0.67	11.85 ± 4.31
b_1 (S)	NSig.	NSig.
b_2 (T)	1.84 ± 0.53	NSig.
b_{12} (S × T)	NSig.	NSig.
b_{11} (S^2)	NSig.	NSig.
b_{22} (T^2)	−2.73 ± 0.56	−4.88 ± 3.67
R^2	0.683	0.505
R^2_{adj}	0.620	0.460
F1	10.78	11.24
	$[F^2_{10} = 4.10] \Rightarrow$ Sig.	$[F^1_{11} = 4.84] \Rightarrow$ Sig.
F2	0.362	0.212
	$[F^8_2 = 19.37] \Rightarrow$ Sig.	$[F^8_1 = 238.9] \Rightarrow$ Sig.
F3	12.70	1.26
	$[F^{10}_4 = 5.96] \Rightarrow$ NSig.	$[F^{11}_4 = 5.94] \Rightarrow$ Sig.
F4	20.50	1.40
	$[F^6_4 = 6.16] \Rightarrow$ NSig.	$[F^7_4 = 6.09] \Rightarrow$ Sig.
S_{opt}	> 37	Not affected
T_{opt} (°C)	20.6	19.0
Y_{max} (as N/N_0)	7.68	11.9

between simulated and experimental data) falling within a range of 70–95% for R^2_{adj} and 75–96% for R^2 was observed. Best agreement was found with *D. caudata* (Tables 6 & 7).

The consistency of the equations was demonstrated in all situations (*F1*, *F2* and *F3* were always confirmed; *F4* in 5 of the 6 cases). The convex pattern obtained by the quadratic and negative terms of T in all *Dinophysis* spp., and also for S in *D. acuta*, indicated a clear maximum N/N_0 close to the centre of the experimental domain for T. Using numerical derivatives of the equations (Wardhani et al. 2010), optimal conditions of T and S that maximized growth in the exponential phase and yield (biomass) in the stationary phases were calculated: 19°C/>37 and 16.7°C/>37 for *D. acuminata*; 17.9°C/29.3 and 16.8°C/28.7 for *D. acuta*; and 20.6°C/>37 and 20.8°C/>37 for *D. caudata* (Table 6).

A. minutum showed similar behaviour with a parabolic pattern for T, but low or null effect for S (Table 7). Values estimating the accuracy of the fits (experimental versus predicted data) were lower (R^2 = 0.505–0.683 and R^2_{adj} = 0.460–0.620) than those obtained with *Dinophysis* spp. cultures. The optimal values of T for maximum yield (biomass) were in the range of 19.0–20.6°C and with a limited influence of S.

3.4. Toxin production and accumulation in *Dinophysis* spp.

A 6 d lag phase was observed in *D. acuminata* and *D. acuta* with the 2 T/S treatments (12.5°C/21 and 12.5°C/35) used in Expt 2 (Fig. 4), but toxin produc-

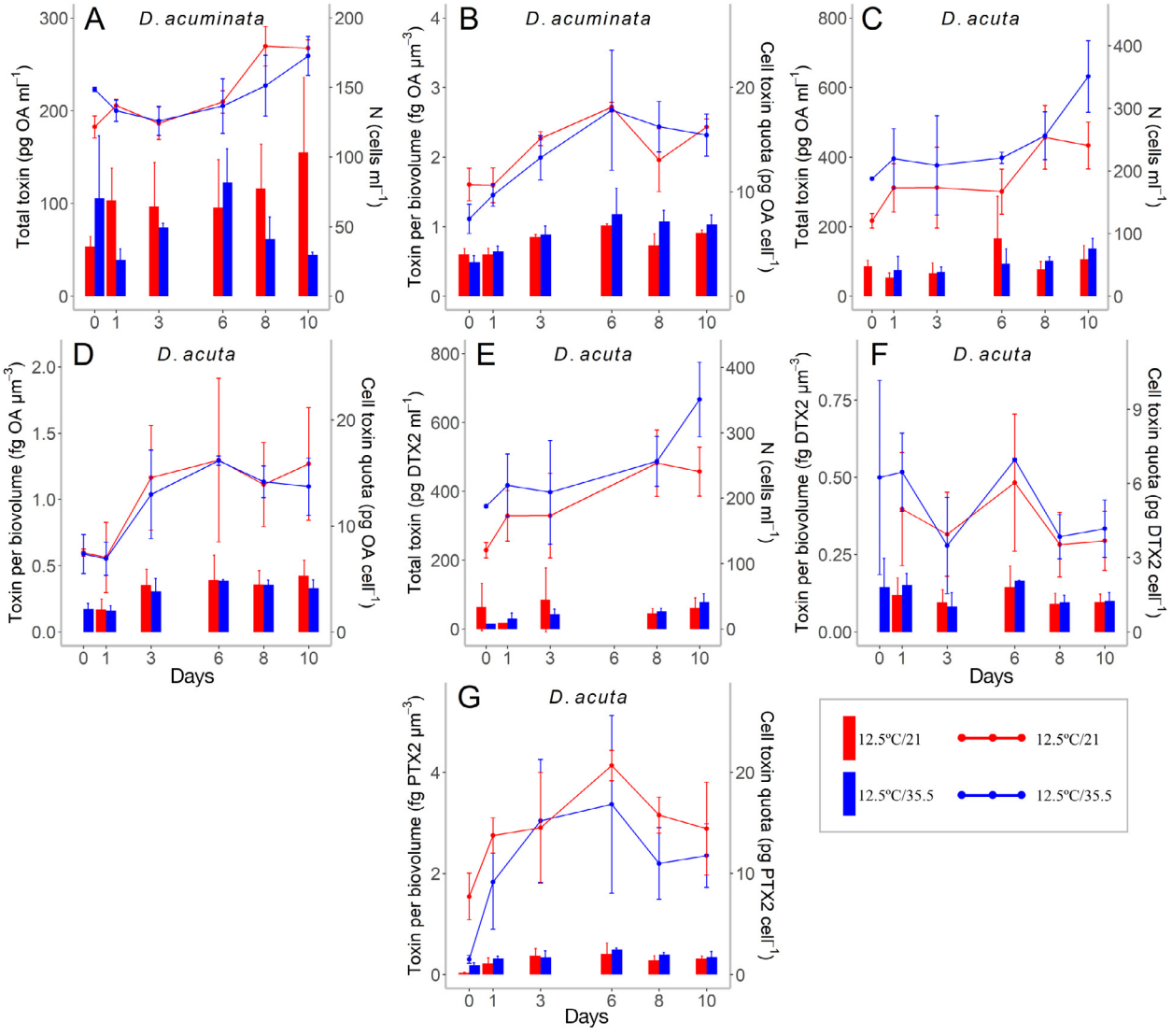

Fig. 4. Population (N) growth curves (cells ml^{-1}), total (particulate + disolved) culture toxin content (pg toxin ml^{-1}) and toxin per cell (pg toxin cell^{-1}) and per biovolume (fg toxin µm^{-3}) of *Dinophysis* spp. under 2 different temperature and salinity (T/S) treatments: 12.5°C/21 (red) and 12.5°C/35.5 (blue): (A) *D. acuminata* growth curve and total okadaic acid (OA) per ml of culture (bar graph); (B) *D. acuminata* OA per cell (pg cell^{-1}) (curve) and per biovolume (fg µm^{-3}) (bar graph); (C) *D. acuta* growth curve and total OA per ml of culture (bar graph); (D) *D. acuta* per cell (pg OA cell^{-1}) (curve) and per biovolume (fg µm^{-3}) (bar graph); (E) *D. acuta* growth curve and total dinophysistoxin 2 (DTX2) per ml of culture (bar graph); (F) *D. acuta* DTX2 per cell (pg cell^{-1}) (curve) and per biovolume (fg µm^{-3}) (bar graph); (G) *D. acuta* pectenotoxin 2 (PTX2) per cell (pg cell^{-1}) (curve) and per biovolume (fg µm^{-3}) (bar graph). Error bars correspond to standard deviation (SD)

tion was not arrested during that period (Fig. 4A,C). Analyses of the cell extracts by LC-HRMS revealed the presence of the main toxins conforming to the toxin profile of *D. acuminata* (OA) and *D. acuta* (OA, DTX2, PTX2).

3.4.1. Particulate toxins in *Dinophysis* spp.

For *D. acuminata*, significant differences (Wilcoxon test) were not found either between the OA per cell grown with S of 21 and 35.5 ($\rho = 0.568$), or with the OA per biovolume unit ($\rho = 0.351$) (Fig. 4B).

For *D. acuta*, median OA and DTX2 content with S of 21 were slightly lower than with 35.5 ($\rho = 0.78$ and 0.33, respectively) (Fig. 4D), but very similar when expressed per unit of biovolume ($\rho = 0.590$) (Fig. 4F). Differences concerning PTX2 were more pronounced, slightly lower with S of 21 than with 35.5 ($\rho = 0.090$) and the same observed per unit of biovolume ($\rho = 0.170$) (Fig. 4G), but still non-significant. Considering the total toxin content per cell, i.e. OA + DTX2 + PTX2

in *D. acuta*, the same common trend was observed. Median total toxin contents were 28.5 and 31.9 pg cell^{-1} with S of 21 and 35.5, respectively.

The main difference between the 2 species was found in the amount of OA per biovolume: *D. acuminata* showed a content of OA per biovolume unit almost 3 times higher than *D. acuta* (Fig. 4B,D). Differences were lower when considering total toxins (OA + DTX2 + PTX2) in *D. acuta*, which reached maximal values on Day 6, of 56 and 45 pg cell^{-1} with S of 21 and 35, respectively (ρ = 0.576).

3.4.2. Extracellular toxins in *Dinophysis* spp.

Small differences were found in the extracellular concentration of DSTs (OA, DTX2) between different T/S treatments (12.5°C/21, 12.5°C/35.5) and species.

D. acuminata showed a higher concentration of extracellular toxins with S at 21 than at 35.5 (Fig. 4A), whereas the opposite was found in *D. acuta* (Fig. 4C). However, differences (Wilcoxon test) were not statistically significant either for *D. acuminata* (ρ = 0.097) or for *D. acuta* (ρ = 0.3310). Likewise, extracellular concentrations of DTX2 in *D. acuta* were slightly higher with S of 21 (median 44.18) than with 35.5 (Fig. 4E), but not significantly different (ρ = 0.8938). Only trace amounts of extracellular PTX2 were detected.

The proportion of toxins found in the extracellular fraction was very low in both species and treatments. For *D. acuminata*, these proportions were 1–8% (max. on Day 0) with S of 35.5 and 4–7% (max. on Day 1) at S of 21, and for *D. acuta*, 2–8% of the total (max. on Day 6) at S of 21 and 2–5% (max. on Day 1) at S of 35.5 (Fig. 5).

3.4.3. Total toxin (particulate + extracellular) production rates and per cell contents in *Dinophysis* spp.

For *D. acuminata*, total OA (particulate + extracellular) production rates between Days 1 and 6 (1.62 ± 0.26 pg with S 21 and 1.75 ± 0.05 pg OA cell^{-1} d^{-1} with S at 35.5) were very similar (Fig. 5A,B). Differences in daily production rates of OA in *D. acuminata* with S of 21 and

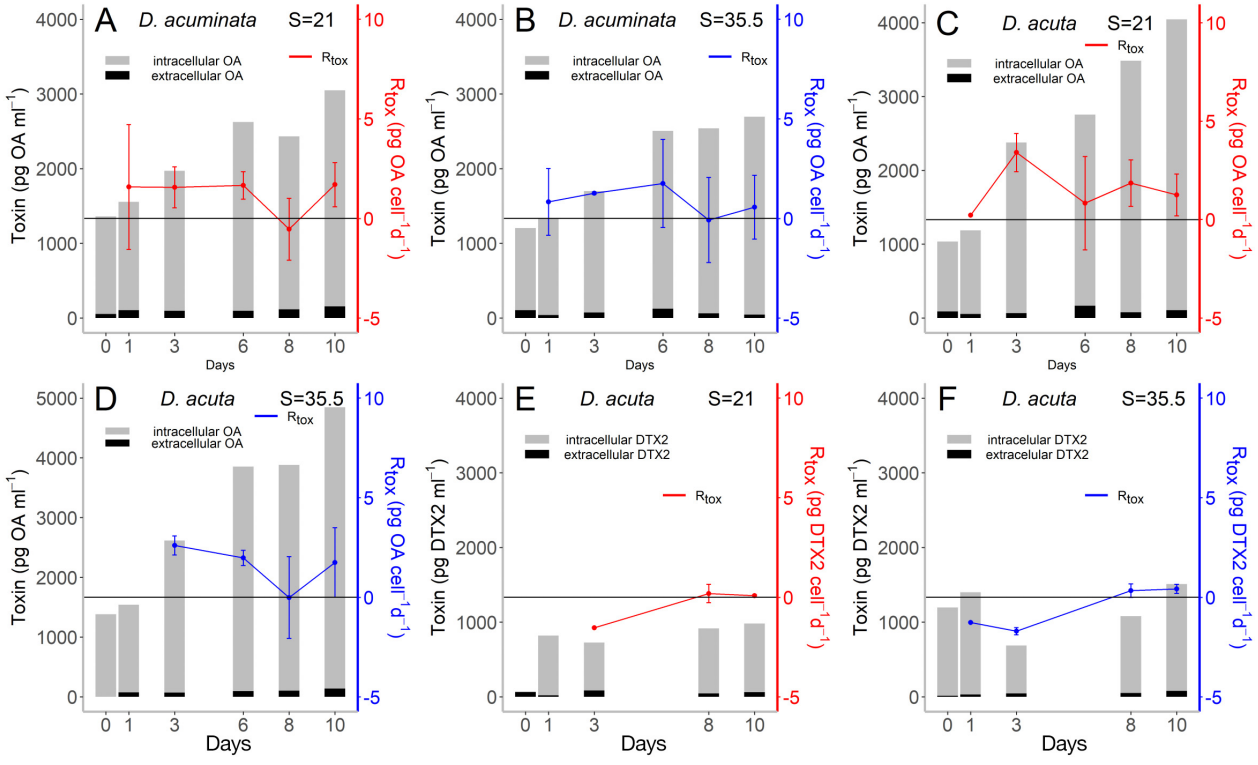

Fig. 5. Particulate and extracellular values (pg ml^{-1}) (bar graphs) and total toxin production rates (R_{tox}, pg OA cell^{-1} d^{-1}) (curves) for (A) *Dinophysis acuminata* okadaic acid (OA) at salinity (S) of 21 (red curve); (B) *D. acuminata* OA at S of 35.5 (blue curve); (C) *D. acuta* OA at S of 21 (red curve); (D) *D. acuta* OA at S of 35.5 (blue curve); (E) *D. acuta* dinophysistoxin 2 (DTX2) at S of 21 (red curve); (F) *D. acuta* DTX2 at S of 35.5 (blue curve)

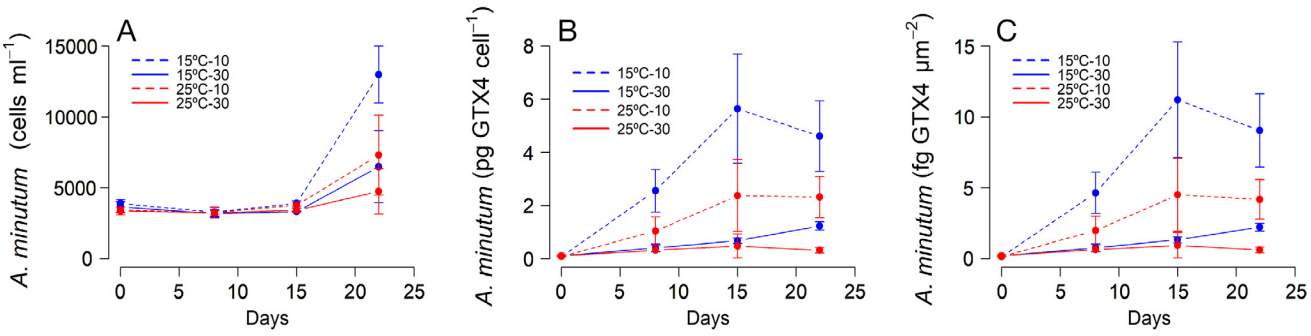

Fig. 6. Growth and cell-toxin curves of *Alexandrium minutum* under 4 different combinations of temperature and salinity (T/S): 15°C/10, 15°C/30, 25°C/10 and 25°C/30. (A) Growth; (B) GTX4 (pg cell^{-1}); (C) GTX4 toxin per biovolume. Error bars represent standard deviation (SD)

35.5, with medians of 0.87 and 0.79 pg OA cell^{-1} d^{-1}, respectively (Fig. 5A,B), were not significant ($\rho = 0.525$).

For *D. acuta*, total OA production rates with S at 21 (1.60 ± 0.28 pg OA cell^{-1} d^{-1}) and at 35.5 (1.41 ± 0.07 pg OA cell^{-1} d^{-1}) (Fig. 5C,D) were not significantly different ($\rho = 0.728$), nor were the total DTX2 production rates (0.08 ± 0.05 pg cell^{-1} d^{-1} with S of 21 and 0.12 ± 0.04 with S 35.5) ($\rho = 0.757$, Fig. 5D–F). In *D. acuta*, 1–12% of the toxins appeared in the dissolved fraction in both treatments. Dissolved toxins were 2–12% of the total at S of 21 (max. on Day 3) and 1–6% at S of 35.5 (max. on Day 3; Fig. 5E,F).

3.5. Toxins in *Alexandrium minutum*

Toxin results showed significantly higher GTX4 quota with S of 10 than with 30. In contrast, no effects on toxin production were observed associated with the T values assayed (Fig. 6). The maximum toxin quota (5.96 pg GTX4 cell^{-1}) was observed with T/S 15°C/10 and the lowest value (3.11 pg GTX4 cell^{-1}), about one-half the maximum, at 15°C/30.

4. DISCUSSION

Our experimental results showed that Galician strains of *Dinophysis* spp. had a narrow range of tolerance to drastic changes in S, whereas *Alexandrium minutum* strains tolerated all T/S combinations assayed. In the Galician Rías, fast-changing T/S conditions are common after wind reversals to upwelling-promoting northerly winds (T stress) or relaxation and downwelling associated with southerly winds and heavy rainfall (S stress), in particular towards the end of the upwelling season (Alvarez-Salgado et al. 2002, Alvarez et al. 2005).

4.1. Effect of T and S stress on *Dinophysis* spp. growth and toxins

Intrinsic biotic factors (physiological status and genetic characteristics of the target species and quality of prey) as well as the size and shape of the experimental vessel are important when comparing the effect of different stressors on microalgal growth and toxicity (Kamiyama et al. 2010, Borowitzka 2018).

Our bifactorial experiment showed that (1) *D. acuminata* and *D. acuta* did not tolerate extremely low S (5–9.7) and *D. acuminata* did not survive at T ≥ 25.5°C; (2) *D. caudata* did not grow at S ≤ 21, but a few cells survived for 10–20 d; and (3) *Dinophysis* species were sensitive to low S, but the effect of S interacted with T.

In the field, seawater density is a function of T and S, and T covaries with S and light (intensity and quality) along a vertical axis from surface to bottom. This may explain why the lower bound of S (21) was tolerated by *D. acuminata* and *D. acuta* only if combined with T ≤ 19°C. The differing responses of the 3 species studied were reflected in the statistical significance of T/S variables: both had the same influence in *D. acuminata*, S had a larger influence than T in *D. acuta* and this effect was even stronger in *D. caudata*.

In a multifactorial (T, S, light intensity) growth experiment with *D. acuminata* from Chesapeake Bay (Fiorendino et al. 2020), T/S interactions at different light intensities were observed, but growth was halted when T was raised to 27°C. In our *D. acuminata* experiments, maximal growth was observed at T/S 19°C/37, and cultures with T ≥ 25.5°C collapsed. Despite the different setup in the 2 studies, common observations included the limited effect of T on population growth within the strain's range of tolerance and the fact that higher T (above 25.5 and 27°C with

Galician and North American strains, respectively) were more stressing for *Dinophysis* spp. growth than the lower bound assayed (12°C).

The above results from multifactorial experiments differ from those in well-fed cultures of *D. acuminata* with a single variable (e.g. T) assayed (Kamiyama et al. 2010, Basti et al. 2018). A significant linear relationship between growth and T (20–26°C) was found during the exponential phase of *D. acuminata* from Harima-Nada, Seto Inland Sea (W Japan, ~34° 30′ N) (Basti et al. 2018), with the same species from a lower latitude (Inokushi Bay, 32° 80′ N) using 4 levels of T (10, 14, 18 and 22°C) (Kamiyama et al. 2010) and with a *D. caudata* strain from Nagasaki (SW Japan ~32° 45′ N), between 15 and 32.5°C (Basti et al. 2015). *D. caudata*, a warm-water species, showed its μ_{max} at 27–30°C, and declined when T reached 32.5°C.

In field populations of *Dinophysis* spp., toxin per cell in individually picked cells or estimates from analyses of net-tows rich in a particular species of *Dinophysis* spp. were the common toxin-related parameters estimated (Fux et al. 2011). MacKenzie et al. (2004) found that a large proportion of *D. acuta* toxins were released in the seawater during late bloom stages and could be adsorbed onto *in situ* passive samplers (SPATT resins). The term 'dissolved' was used to nominate the toxin fraction that went through 0.22 µm pore-size filters. A follow-up in the Galican Rías with weekly deployed SPATT resins showed maximum levels of released toxins during the early stationary phase of *D. acuta* blooms. However, released toxins could also be adsorbed onto mucilage, debris and other organic matrices and detected in haul samples when *D. acuta* cells were no longer present, and PTX2 was more persistent in seawater than the okadaates (Pizarro et al. 2008, 2009). In laboratory cultures, adsorbing resins allow quantification of total toxin (particulate + dissolved fractions) and estimates of production rates. Differences in toxin production rates and cellular content in *D. acuminata* and *D. acuta* grown at 12.5°C with S of 21 or 35.5 were not significant in our experiments. The most relevant observation, common to *D. acuminata* and *D. acuta*, was that until Day 6, when the cells were under T/S stress and growth was arrested, toxin production continued, and declined slightly when moderate growth resumed. Tong et al. (2011) found maximal toxin per cell in stationary cultures of *D. acuminata* and stated that toxins were differentially produced or accumulated during different growth phases. These results agree with observations of *D. acuta* field populations in the Galician Rías, i.e. the highest values of toxin per cell were observed before bloom decline in advected populations with no active division, and different patterns of production and persistence in the 2 main groups (OAs and PTXs) of toxins (Pizarro et al. 2008, 2009). In the Celtic Sea, southwest Ireland, *D. acuta* cells from different depths, even those found at 80 m, had similarly high contents of OA, DTX2 and PTXs (Fux et al. 2010).

These observations confirm the distinct responses of each toxin group (OAs, PTXs) and of cellular division in mixotrophic *Dinophysis* spp. under different T/S conditions. A transient increase of cellular toxin quota is due to accumulation as a result of uncoupling between toxin production (that continues) and cellular division (that stops).

The very low ratios of extracellular OA found contrasts with the high ratios of OA + DTX1 (79.5%) and low ratios of PTX (5.1%) in stationary well-fed cultures of *D. acuminata* and *D. fortii* (Nagai et al. 2011). Nielsen et al. (2013) found that extracellular toxins (up to 90% of the production) comprise a higher percentage in well-fed than in starved cultures of *D. acuta*, where percentages (up to 22%) increased initially at the beginning but declined later. These results, in addition to our observations, suggest that release of extracellular OA-related toxins in *Dinophysis* spp. cultures should not be interpreted as a sign of stress, but as a normal process in aged populations.

4.2. Effect of T and S stress on *Alexandrium minutum* growth and toxin content

A. minutum tolerated all S values within the range tested, and the most limiting factor for growth was T. High cell densities were reached in cultures at 23.6°C and S values between 9.7 and 32.3.

A. minutum is considered a euryhaline species. Grzebyk et al. (2003) reported positive growth in a strain from Brittany (Atlantic coast, France, ~48° N) with S values 12–37, and μ_{max} was observed at 25. Toxin per cell was 5-fold higher (50 pg cell^{-1}) at S of 15 and $\mu = 0.28$ d^{-1} than at S of 37 (10 pg cell^{-1}) with $\mu = 0.48$ d^{-1}. Toxin production (fg GTX cell^{-1} d^{-1}) was maximal in the late exponential phase, and the high content per cell with low S was interpreted as toxin accumulation due to the imbalance between growth and toxin production.

The strain from Baiona Bay (~42° N) used in our experiments showed exponential growth at T between 19 and 23.6°C. Independently of T conditions, cultures maintained a stable population with a flattened curve. GTX4 content per cell was highest at

the lowest S tested (30 versus 10 fg cell^{-1}, $\rho = 0.005$) but T effects on cell toxin quota were not significant. These results agree with those obtained with the French strain, i.e. *A. minutum* toxin content tends to be higher at lower S values (Grzebyk et al. 2003, Lim & Ogata 2005). Results from the present study suggest that in the *A. minutum* strains from Galicia and Brittany, the enzymatic pathways involved in toxin production, as well as growth, are adapted to low-S environments.

S stress affects the osmotic balance of cells. Their response to restore it may include the synthesis of osmolyte molecules in addition to physiological adjustments such as reduction (or even inhibition) of growth and photosynthesis rates (Kirst 1990, Borowitzka 2018). Different physiological adaptations in response to produce these osmolytes may explain the response of *Dinophysis* spp., more affected by S stress, in contrast with *A. minutum*, which showed a clear pattern of higher toxin content in cultures with lower S and higher μ (Fig. 6).

4.3. Effect of T and S stress on *Dinophysis* spp. shape and size

Small gamete-like cells formed through a depauperating division of mature cells constitute a stage in the sexual life cycle of *Dinophysis* spp. populations (Reguera & González-Gil 2001). Small cell formation is a normal process in natural healthy populations of *Dinophysis* spp. Various authors have followed the relative abundance of these cells during bloom development of *D. acuta* in the Galician Rías (Reguera et al. 1995), northern Portugal (Moita et al. 2006) and New Zealand (MacKenzie 1992); of *D. acuminata* in the Baltic Sea (Hajdu & Larsson 2006) and Galicia (Escalera & Reguera 2008); *D. caudata* in the Ebro Delta (Mediterranean Sea) (Delgado et al. 2000); and *D. ovum* in Thermaikos Bay, Greece (Koukaras & Nikolaidis 2004), and Texas, Gulf of Mexico (Campbell et al. 2010). The common observation was that small cells may always be present, comprising 1–5% of the population, but higher percentages are observed during the last phases (late exponential to stationary) of population growth. Exceptionally high percentages (>40%) of small cells were reported by MacKenzie (1992) and Hajdu & Larsson (2006). These forms were also observed after incubations of field isolated cells on culture plates (Reguera 2003, Escalera & Reguera 2008), but nonviable small cells appeared also in failed attempts to isolate and culture *D. caudata*. Koike et al. (2006) concluded that sexual reproduction in *D. fortii* would allow survival under stress conditions, while aberrant cells are possibly an artifact product from laboratory culture conditions.

In our experiments, maximal percentages of small (*D. dens*-like) cells of *D. acuta* were observed in the decline phase, 5 d after the cell maximum was reached, and of small (*D. diegensis*-like) cells of *D. caudata* during the exponential phase. There are no experimental data to support the hypothesis that small cell formation in mixotrophic species of *Dinophysis* is triggered by nutrient limitation. In any case, they did not seem to be associated with a quick response of *D. acuta* or *D. caudata* to environmental stress in the present study.

Aberrant cells appeared in cultures of *D. acuta* but a high proportion (18.6% of total cells) was only found in the 23.6°C/32.3 T/S treatment after weeks of cultivation. These forms, in agreement with Koike et al. (2005), are most likely laboratory artefacts. The percentage of aberrant cells observed in the other treatments was very small (<2.5%).

4.4. Ecological implications

Results from the present study allowed us to delimit windows of tolerance for T and S, and the weight of both variables in some of the most frequent HAB species in the Galician Rías. The optimal common treatment was T/S 19°C/37. These results also confirmed a frequent observation in laboratory experiments, i.e. optimal microalgal growth occurs at T much higher than those met in their habitat. Nevertheless, field populations affected by multiple factors attain their maximum growth at depths that represent a trade-off for optimal biotic and abiotic conditions (Litchman et al. 2015). Thus, *D. acuta* and *D. caudata* population maxima would be located farther offshore where summer S values are quite stable (~35.5), and *D. acuta* in deeper, colder and less illuminated water layers than *D. caudata* (Díaz et al. 2016, 2019a). In turn, *A. minutum* may grow at the same time within small embayments that avoid dynamic exchanges with shelf waters (upwelling shadows) (Bravo et al. 2010).

The optimal windows of T and S for *Dinophysis* spp. and *A. minutum* in the Galician Rías may be different for strains of the same species in other coastal systems and/or latitudes. *A. minutum*'s ability to withstand highly variable S (Grzebyk et al. 2003) explains its capacity to bloom in brackish tropical Kingston Bay, Jamaica (~18° N), with S of 11 and T at 26.5°C

(Ranston et al. 2007), as well as hypersaline (Gulf of Gabes, Tunisia, SW Mediterranean, ~34° N) with S of 36.7–44, and T of 19–23.6°C in coastal lagoons (Abdenadher et al. 2012). The optimal T/S levels appear to vary according to the geographic location, associated with local adaptation. For all the above, *A. minutum* as a whole would be able to thrive in a range of environments if initial introductions are able to survive while adaptation takes place (Lewis et al. 2018).

Large differences in T/S tolerance reflect regional adaptations of *Dinophysis* strains of the species studied here to environmental conditions. For example, in the Patagonian Fjords, southern Chile (41–46° S), a *D. acuminata* maximum was observed in a thin layer at 16.1–16.5°C and S between 17.4 and 20 (Baldrich et al. 2021), but scattered populations in the same region tolerated S values from 5 to 20 (Díaz et al. 2011, Alves de Souza et al. 2019). Co-occurring blooms of *D. acuta* were found in slightly deeper, saltier (S of 23–25) waters (Baldrich et al. 2021). In the Baltic Sea, *D. acuminata* occurs in a wide range of T (4.4–20°C) and very low S (5.5–6.9) (Hallfors et al. 2011).

Different T/S ranges of tolerance in our study help understand the environmental conditions promoting/excluding bloom development in the Galician Rías and identify common features within strains of the same species in different systems. *D. acuminata* is a coastal species that occurs from spring to autumn under a wider range of T and S than *D. acuta*, a mid-shelf water species with a shorter (late summer-early autumn) growth season. *D. acuminata* growth starts at the onset of spring thermohaline stratification, whereas *D. acuta* requires marked thermal stratification and stability (hot and dry summers) (Escalera et al. 2010, Raine et al. 2018). In Chilean fjords, strong S gradients are always present. There, *D. acuminata* growth starts when late spring solar heating overturns the winter-early spring thermal inversion caused by river outflow and ice melt. *D. acuta* blooms follow when thermal stratification becomes stronger (Alves de Souza et al. 2019, Díaz et al. 2021).

In the Galician Rías, during a 36 h fine-scale sampling at the beginning of a short-term upwelling cycle (3–14 d time scales), a thin layer of diatoms rose from 18 to 10 m in 26 h, and T in the top layer fell more than 2°C in 5 h (Díaz et al. 2019b). These changes were associated with a decline in specific growth (μ, from 0.65 to 0.33 d^{-1}) of a *D. acuminata* population located in the top 5 m. Thus, in addition to the population dispersal with intensified outflow at the surface, upwelling may indirectly contribute to the decline of dinoflagellate populations, in particular mixotrophic species of *Dinophysis*, due to the negative effect of abrupt cooling on division rates.

In the Galician Rías and adjacent shelf, *D. caudata* is a late mid-shelf summer-autumn species, co-occurring with or following *D. acuta*, and only exceptionally exceeding levels of 10^3 cells l^{-1}. Indeed, our experiments reflected *D. caudata* flexibility to higher T and S than the other 2 *Dinophysis* species. This warm water species proliferates in tropical-subtropical systems (Larsen & Moestrup 1992) and on western Mediterranean coasts (Zingone et al. 2021). There, during a persistent occurrence of this species in the Ebro Delta bays (NE Spain, ~41° N), conditions during the population maximum were 24°C and S of 35 (Delgado et al. 2000).

The variegated response of each harmful dinoflagellate species to increased T in a multifactorial scenario shows that it is not a simple linear response within an optimal environmental window for growth. Each species adapts to differently structured (S- or T-driven) water columns; if the species co-occur, their maxima are at different depths. In upwelling systems, anticyclonic weather brings dry and warmer air but also upwelling of colder water near the surface. In fjords, increased air temperatures in spring enhance ice melt and flushing rates by cold water. In the case of *Dinophysis* spp., the 2 systems allow its development when thermal gradients are formed. Thus, the effects of climate variation cannot be modelled or forecast on the basis of a single parameter ignoring multifactorial effects, including S, on the individual species.

5. CONCLUSIONS

The response of 3 species of *Dinophysis* and *Alexandrium minutum* to T and S stress and their windows of tolerance reflected their specific adaptations to these variables. The 4 species may co-occur in time in the Galician Rías, each one occupying different environmental niches. The range of tolerance to T stress of the 2 temperate-water species of *Dinophysis* (*D. acuminata* and *D. acuta*) and *A. minutum* were well above the range observed in their local habitat. These differences highlight deep adaptive traits in these organisms and their resilience under short-term changing environmental conditions within their ecological niches in the upwelling system of the Galician Rías. These results are highly relevant to model their responses under variable physical-chemical conditions, in order to develop predictive models and advance our understanding about their spatial-temporal trends in the area.

Acknowledgements. We are grateful to Dr. David Jaen (LCCRRPP, Junta de Andalucía, Spain) for sharing his cultures of *Teleaulax amphioxeia* (AND-A070) and *Mesodinium rubrum* (AND-A0711), and our colleagues Dr. Fernando Rayón and Hortensia Araujo (IEO-CSIC) for their help in preparing the graphs. This work was funded by the EU-INTERREG Atlantic Area project PRIMROSE (EAPA 182/2016) and a GAIN grant from the Innovation Agency of the Galician Government (Xunta de Galicia) for Galician Networks of Excellence (GRC-VGOHAB IN607A-2019/04), with the support of the CCVIEO Culture Collection of Microalgae from the Oceanographic Centre of Vigo (IEO, CSIC). M.S. acknowledges a pre-doctoral contract granted to the Spanish project DIANAS (CTM2017-86066-R), RETOS Programme, MINECO. This work is a contribution of the Unidad Asociada de Microalgas Nocivas-VGOHAB group-IEO-CSIC.

LITERATURE CITED

Abdenadher M, Hamza A, Fekih W, Hannachi I, Bellaaj AZ, Bradai MN, Aleya L (2012) Factors determining the dynamics of toxic blooms of *Alexandrium minutum* during a 10-year study along the shallow southwestern Mediterranean coasts. Estuar Coast Shelf Sci 106:102–111

Akhnazarova S, Kafarov V (1982) Experiment optimization in chemistry and chemical engineering. MIR Publishers, Moscow

Alvarez I, deCastro M, Gomez-Gesteita M, Prego R (2005) Inter- and intra-annual analysis of the salinity and temperature evolution in the Galician Rías Baixas–ocean boundary (northwest Spain). J Geophys Res Oceans 110: C04008

Alvarez-Salgado XA, Beloso S, Joint I, Nogueira E and others (2002) New production of the NW Iberian shelf during the upwelling season over the period 1982–1999. Deep Sea Res I 49:1725–1739

Alves de Souza C, Iriarte JL, Mardones JI (2019) Interannual variability of *Dinophysis acuminata* and *Protoceratium reticulatum* in a Chilean fjord: insights from the realized niche analysis. Toxins 11:1–19

Baldrich AM, Perez-Santos I, Alvarez G, Reguera B and others (2021) Niche differentiation of *Dinophysis acuta* and *D. acuminata* in a stratified fjord. Harmful Algae 103: 102010

Balech E (2002) Dinoflagelados tecados tóxicos del Cono Sur Americano. In: Sar EA, Ferrario ME, Reguera B (eds) Floraciones algales nocivas en el Cono Sur Americano. Instituto Español de Oceanografía, Madrid, p 123–144

Basti L, Uchida H, Matsushima R, Watanabe R, Suzuki T, Yamatogi T, Nagai S (2015) Influence of temperature on growth and production of pectenotoxin-2 by a monoclonal culture of *Dinophysis caudata.* Mar Drugs 13: 7124–7137

Basti L, Suzuki T, Uchida H, Kamiyama T, Nagai S (2018) Thermal acclimation affects growth and lipophilic toxin production in a strain of cosmopolitan harmful alga *Dinophysis acuminata.* Harmful Algae 73:119–128

Belin C, Soudant D, Amzil Z (2021) Three decades of data on phytoplankton and phycotoxins on the French coast: lessons from REPHY and REPHYTOX. Harmful Algae 102:101733

Ben-Gigirey B, Rossignoli AE, Riobo P, Rodriguez F (2020) First report of paralytic shellfish toxins in marine invertebrates and fish in Spain. Toxins 12:723

Blanco J, Mariño J, Campos MJ (1985) The first toxic bloom of *Gonyaulax tamarensis* detected in Spain. In: Anderson DM, White AW, Baden DG (eds) Toxic dinoflagellates. Elsevier, New York, NY, p 8–12

Blanco J, Moroño A, Fernández ML (2005) Toxic episodes in shellfish produced by lipophilic phycotoxins: an overview. Rev Gal Rec Mar 1:1–70

Borowitzka M (2018) The 'stress' concept in microalgal biology — homeostasis, acclimation and adaptation. J Appl Phycol 30:2815–2825

Box GE, Hunter JS, Hunter WG (2005) Statistics for experimenters: design, innovation, and discovery. John Wiley & Sons, New York, NY

Boyd PW, Rynearson TA, Armstrong EA, Fu F and others (2013) Marine phytoplankton temperature versus growth responses from polar to tropical waters — outcome of a scientific community-wide study. PLOS ONE 8:e63091

Bravo I, Fraga S, Figueroa RI, Pazos Y, Massanet A, Ramilo I (2010) Bloom dynamics and life cycle strategies of two toxic dinoflagellates in a coastal upwelling system (NW Iberian Peninsula). Deep Sea Res II 57:222–234

Bresnan E, Arevalo F, Belin C, Branco MAC and others (2021) Diversity and regional distribution of harmful algal events along the Atlantic margin of Europe. Harmful Algae 102:101976

Campbell L, Olson RJ, Sosik HM, Abraham A, Henrichs DW, Hyatt CJ, Buskey EJ (2010) First harmful *Dinophysis* (Dinophyceae, Dinophysiales) bloom in the U.S. is revealed by automated imaging flow cytometry. J Phycol 46:66–75

Carstensen J, Klais R, Cloern JE (2015) Phytoplankton blooms in estuarine and coastal waters: seasonal patterns and key species. Estuar Coast Shelf Sci 162:98–109

Delgado M, Santmarti M, Vila M, Garcés E, Camp J (2000) Seguimiento del fitoplancton tóxico en las bahías del Delta del Ebro en los años 1997–1998. In: Junta de Andalucía CdAyP (ed) Proc VI Reunión Ibérica sobre Fitoplanctón Tóxio y Biotoxinas. Congresos y Jornada Sevilla 55/00:51–58

Díaz P, Molinet C, Caceres MA, Valle-Levinson A (2011) Seasonal and intratidal distribution of *Dinophysis* spp. in a Chilean fjord. Harmful Algae 10:155–164

Díaz PA, Reguera B, Ruiz-Villarreal M, Pazos Y, Velo-Suarez L, Berger H, Sourisseau M (2013) Climate variability and oceanographic settings associated with interannual variability in the initiation of *Dinophysis acuminata* blooms. Mar Drugs 11:2964–2981

Díaz PA, Ruiz-Villarreal M, Pazos Y, Moita T, Reguera B (2016) Climate variability and *Dinophysis acuta* blooms in an upwelling system. Harmful Algae 53:145–159

Díaz PA, Reguera B, Moita T, Bravo I, Ruíz-Villarreal M, Fraga S (2019a) Mesoscale dynamics and niche segregation of two *Dinophysis* especies in Galician-Portuguese coastal waters. Toxins 11:37

Díaz PA, Ruiz-Villarreal M, Mourino-Carballido B, Fernandez-Pena C, Riobo P, Reguera B (2019b) Fine scale physical–biological interactions during a shift from relaxation to upwelling with a focus on *Dinophysis acuminata* and its potential ciliate prey. Prog Oceanogr 175:309–327

Díaz PA, Peréz-Santos I, Álvarez G, Garreaud R and others (2021) Multiscale physical background to an exceptional harmful algal bloom of *Dinophysis acuta* in a fjord system. Sci Total Environ 773:145621

Egmond HAT, Patrick L, Speijers GJA, Waldock M (1993) Paralytic and diarrheic shellfish poisons: occurrence in

Europe, toxicity analysis and regulation. J Nat Toxins 2: 41–83

Escalera L, Reguera B (2008) Planozygote division and other observations on the sexual cycle of several species of *Dinophysis* (Dinophyceae, Dinophysiales). J Phycol 44: 1425–1436

Escalera L, Reguera B, Moita T, Pazos Y, Cerejo M, Manuel Cabanas J, Ruiz-Villarreal M (2010) Bloom dynamics of *Dinophysis acuta* in an upwelling system: *in situ* growth versus transport. Harmful Algae 9:312–322

European Commission (2021) Commission Delegated Regulation (EU) 2021/1374 of 12 April 2021 amending Annex III to Regulation (EC) No 853/2004 of the European Parliament and of the Council on specific hygiene requirements for food of animal origin (text with EEA relevance). Off J Eur Union L 297:1–15

European Parliament and Council (2004) Regulation (EC) No 853/2004 of the European Parliament and of the Council of 29 April 2004 laying down specific hygiene rules for food of animal origin. Off J Eur Union L 139: 55–205

Fernandes-Salvador JA, Davidson K, Sourisseau M, Revilla M and others (2021) Current status of forecasting toxic harmful algae for the North-East Atlantic shellfish aquaculture industry. Front Mar Sci 8:666583

Fernández M, Delgado M, Vila M, Sampedro N, Camp J, Furones D, Diogène J (2008) Resultados del programa de seguimiento de fitoplancton tóxico y biotoxinas en las zonas se producción de bivalvos de Calaluña: años 2003–2006 y primer trimestre del 2007. In: Gilabert J (ed) Avances y tendencias en fitoplancton tóxico y biotoxinas: Actas IX Reunión Ibérica sobre Fitoplancton Tóxico y Biotoxinas. Javier Gilabert Cervera, Cartagena, p 37–46

Figueroa RI, Vázquez JA, Massanet A, Murado MA, Bravo I (2011) Interactive effects of salinity and temperature on planozygote and cyst formation of *Alexandrium minutum* (Dinophyceae) in culture. J Phycol 47:13–24

Fiorendino JM, Smith JL, Campbell L (2020) Growth response of *Dinophysis*, *Mesodinium*, and *Teleaulax* cultures to temperature, irradiance, and salinity. Harmful Algae 98:101896

Fux E, González-Gil S, Lunven M, Gentien P, Hess P (2010) Production of diarrhetic shellfish poisoning toxins and pectenotoxins at depths within and below the euphotic zone. Toxicon 56:1487–1496

Fux E, Smith JL, Tong M, Guzmán L, Anderson DM (2011) Toxin profiles of five geographical isolates of *Dinophysis* spp. from North and South America. Toxicon 57:275–287

Gaillard S, Réveillon D, Danthu C, Hervé F and others (2021) Effect of a short-term salinity stress on the growth, biovolume, toxins, osmolytes and metabolite profiles on three strains of the *Dinophysis acuminata*-complex (*Dinophysis* cf. *sacculus*). Harmful Algae 107:102009

Garcia-Cuetos L, Moestrup O, Hansen PJ, Daugbjerg N (2010) The toxic dinoflagellate *Dinophysis acuminata* harbors permanent chloroplasts of cryptomonad origin, not kleptochloroplasts. Harmful Algae 9:25–38

GEOHAB (2001) Global ecology and oceanography of harmful algal blooms, science plan. In: Glibert P, Picher G (eds) SCOR and IOC, Baltimore, MD, and Paris

GEOHAB (2011) GEOHAB modelling: a workshop report. In: McGillicuddy DJ, Glibert P, Berdalet E, Edwards C, Franks P, Ross O (eds) SCOR and IOC, Paris and Newark, DE

Glibert PM (2016) Margalef revisited: a new phytoplankton mandala incorporating twelve dimensions, including nutritional physiology. Harmful Algae 55:25–30

Glibert PM (2017) Eutrophication, harmful algae and biodiversity — challenging paradigms in a world of complex nutrient changes. Mar Pollut Bull 124:591–606

Granéli E, Cod GA, Dale B, Lipiatou E, Maestrini SY, Rosenthal H (1999) EUROHAB: harmful algal blooms in European marine and brackish waters. Research in Enclosed Seas Series, EUR 18592, Book 5. European Commission, Luxembourg

Grzebyk D, Bechemin C, Ward CJ, Verite C, Codd GA, Maestrini SY (2003) Effects of salinity and two coastal waters on the growth and toxin content of the dinoflagellate *Alexandrium minutum*. J Plankton Res 25:1185–1199

Guallar C, Bacher C, Chapelle A (2017) Global and local factors driving the phenology of *Alexandriurn minutum* (Halim) blooms and its toxicity. Harmful Algae 67:44–60

Guillard RRL (1973) Division rates. In: Stein J (ed) Handbook of phycological methods; culture methods and growth measurements. Cambridge University Press, Cambridge, p 289–312

Guillard RRL, Hargraves PE (1993) *Stichochrysis immobilis* is a diatom, not a chrysophyte. Phycologia 32:234–236

Hajdu S, Larsson U (2006) Life-cycle stages of *Dinophysis acuminata* (Dinophyceae) in the Baltic Sea. Afr J Mar Sci 28:289–293

Hallfors H, Hajdu S, Kuosa H, Larsson U (2011) Vertical and temporal distribution of the dinoflagellates *Dinophysis acuminata* and *D. norvegica* in the Baltic Sea. Boreal Environ Res 16:121–135

Jeong HJ, Yoo YD, Kim JS, Seong KA, Kang NS, Kim T (2010) Growth, feeding and ecological roles of the mixotrophic and heterotrophic dinoflagellates in marine planktonic food webs. Ocean Sci J 45:65–91

Kamiyama T, Nagai S, Suzuki T, Miyamura K (2010) Effect of temperature on production of okadaic acid, dinophysistoxin-1, and pectenotoxin-2 by *Dinophysis acuminata* in culture experiments. Aquat Microb Ecol 60:193–202

Keller MD, Selvin RC, Claus W, Guillard RR (1987) Media for the culture of oceanic ultraphytoplankton. J Phycol 23:633–638

Kim M, Nam SW, Shin W, Coats DW, Park MG (2012) *Dinophysis caudata* (Dinophyceae) sequesters and retains plastids from the mixotrophic ciliate prey *Mesodinium rubrum*. J Phycol 48:569–579

Kirst GO (1990) Salinity tolerance of eukaryotic marine algae. Annu Rev Plant Physiol Plant Mol Biol 41:21–53

Koike K, Sekiguchi H, Kobiyama A, Takishita K, Kawachi M, Ogata T (2005) A novel type of kleptoplastidy in *Dinophysis* (Dinophyceae): presence of haptophyte-type plastid in *Dinophysis mitra*. Protist 156:225–237

Koike K, Nishiyama A, Saitoh K, Imai K, Koike K, Kobiyama A, Ogata T (2006) Mechanism of gamete fusion in *Dinophysis fortii* (Dinophyceae, Dinophyta): light microscopic and ultrastructural observations. J Phycol 42:1247–1256

Koukaras K, Nikolaidis G (2004) *Dinophysis* blooms in Greek coastal waters (Thermaikos Gulf, NW Aegean Sea). J Plankton Res 26:445–457

Larsen J, Moestrup Ø (1992) Potentially toxic phytoplankton. 2. Genus *Dinophysis* (Dinophyceae). ICES Identification Leaflets for Plankton 180. Plymouth Marine Lab, Plymouth

Lewis AM, Coates LN, Turner AD, Percy L, Lewis J (2018) A review of the global distribution of *Alexandrium minutum* (Dinophyceae) and comments on ecology and asso-

ciated paralytic shellfish toxin profiles, with a focus on Northern Europe. J Phycol 54:581–598
Li AF, Li MH, Qiu JB, Song JL and others (2018) Effect of suspended particulate matter on the accumulation of dissolved diarrhetic shellfish toxins by mussels (*Mytilus galloprovincialis*) under laboratory conditions. Toxins 10:273
Lim PT, Ogata T (2005) Salinity effect on growth and toxin production of four tropical *Alexandrium species* (Dinophyceae). Toxicon 45:699–710
Litchman E, Edwards KF, Klausmeier CA (2015) Microbial resource utilization traits and trade-offs: implications for community structure, functioning, and biogeochemical impacts at present and in the future. Front Microbiol 6: 254
MacKenzie L (1992) Does *Dinophysis* (Dinophyceae) have a sexual life cycle? J Phycol 28:399–406
MacKenzie L, Beuzenberg V, Holland P, McNabb P, Selwood A (2004) Solid phase adsorption toxin tracking (SPATT): a new monitoring tool that simulates the biotoxin contamination of filter feeding bivalves. Toxicon 44:901–918
Margalef R (1978) Life-forms of phytoplankton as survival alternatives in an unstable environment. Oceanol Acta 1: 493–509
Mitra A, Flynn KJ, Tillmann U, Raven JA and others (2016) Defining planktonic protist functional groups on mechanism for energy and nutrient acquisition: incorporation of diverse mixotrophic strategies. Protist 167:106–120
Moita MT, Sobrinho-Goncalves L, Oliveira PB, Palma S, Falcao M (2006) A bloom of *Dinophysis acuta* in a thin layer off north-west Portugal. Afr J Mar Sci 28:265–269
Moore SK, Johnstone JA, Banas NS, Salathe EP Jr (2015) Present-day and future climate pathways affecting *Alexandrium* blooms in Puget Sound, WA, USA. Harmful Algae 48:1–11
Nagai S, Suzuki T, Nishikawa T, Kamiyama T (2011) Differences in the production and excretion kinetics of okadaic acid, dinophysistoxin-1, and pectenotoxin-2 between cultures of *Dinophysis acuminata* and *Dinophysis fortii* isolated from western Japan. J Phycol 47:1326–1337
Nielsen LT, Krock B, Hansen PJ (2013) Production and excretion of okadaic acid, pectenotoxin-2 and a novel dinophysistoxin from the DSP-causing marine dinoflagellate *Dinophysis acuta* — effects of light, food availability and growth phase. Harmful Algae 23:34–45
Nogueira E, Bravo I, Montero P, Díaz-Tapia P and others (2022) HABs in coastal upwelling systems: insights from an exceptional red tide of the toxigenic dinoflagellate *Alexandrium minutum.* Ecol Indic 137:108790
Pazos Y, Moroño A (2008) Microplancton tóxico y nocivo en las Rías Gallegas en los años 2003 a 2006. In: Gilabert J (ed) Avances y tendencias en fitoplancton tóxico y biotoxinas: Actas IX Reunión Ibérica sobre Fitoplancton Tóxico y Biotoxinas. Javier Gilabert Cervera, Cartagena p 13–28
Pease SKD, Brosnahan ML, Sanderson MP, Smith JL (2022) Effects of two toxin-producing harmful algae, *Alexandrium catenella* and *Dinophysis acuminata* (Dinophyceae), on activity and mortality of larval shellfish. Toxins 14:335
Pitcher GC, Figueiras FG, Hickey BM, Moita MT (2010) The physical oceanography of upwelling systems and the development of harmful algal blooms. Prog Oceanogr 85: 5–32
Pitcher GC, Figueiras FG, Kudela RM, Moita T, Reguera B, Ruíz-Villareal M (2018) Key questions and recent research advances on harmful algal blooms in eastern boundary upwelling systems. In: Glibert PM, Berdalet E, Burford MA, Pitcher GC, Zhou M (eds) Global ecology and oceanography of harmful algal blooms. Ecological studies: analysis and synthesis, Book 232. Springer, New York, NY, p 205–227
Pizarro G, Escalera L, Gonzalez-Gil S, Franco JM, Reguera B (2008) Growth, behaviour and cell toxin quota of *Dinophysis acuta* during a daily cycle. Mar Ecol Prog Ser 353: 89–105
Pizarro G, Paz B, González-Gil S, Franco JM, Reguera B (2009) Seasonal variability of lipophilic toxins during a *Dinophysis acuta* bloom in Western Iberia: differences between picked cells and plankton concentrates. Harmful Algae 8:926–937
Raine R, Berdalet E, Yamazaki H, Jenkinson I, Reguera B (2018) Key questions and recent research advances on harmful algal blooms in stratified systems. In: Glibert PM, Berdalet E, Burford MA, Pitcher GC, Zhou M (eds) Global ecology and oceanography of harmful algal blooms. Ecological studies: analysis and synthesis, Book 232. Springer, New York, NY, p 165–186
Ranston ER, Webber DF, Larsen J (2007) The first description of the potentially toxic dinoflagellate, *Alexandrium minutum* in Hunts Bay, Kingston Harbour, Jamaica. Harmful Algae 6:29–47
Reguera B (2003) Biología, autoecología y toxinología de las principales especies del género *Dinophysis* asociadas a episodios de intoxicación diarreogénica por bivalvos (DSP). PhD thesis, Universidad de Barcelona
Reguera B, González-Gil S (2001) Small cell and intermediate cell formation in species of *Dinophysis* (Dinophyceae, Dinophysiales). J Phycol 37:318–333
Reguera B, Bravo I, Fraga S (1995) Autoecology and some life history states of *Dinophysis acuta* Ehrenberg. J Plankton Res 17:999–1015
Reguera B, Velo-Suarez L, Raine R, Park MG (2012) Harmful *Dinophysis* species: a review. Harmful Algae 14: 87–106
Reguera B, Riobó P, Rodríguez F, Díaz P and others (2014) *Dinophysis* toxins: causative organisms, distribution and fate in shellfish. Mar Drugs 12:394–461
Rodríguez F, Garrido JL, Sobrino C, Johnsen G and others (2016) Divinyl chlorophyll *a* in the marine eukaryotic protist *Alexandrium ostenfeldii* (Dinophyceae). Environ Microbiol 18:627–643
Rodríguez F, Riobó P, Crespín GD, Daranas AH and others (2018) The toxic benthic dinoflagellate *Prorocentrum maculosum* Faust is a synonym of *Prorocentrum hoffmannianum* Faust. Harmful Algae 78:1–8
Rountos KJ, Kim JJ, Hattenrath-Lehmann TK, Gobler CJ (2019) Effects of the harmful algae, *Alexandrium catenella* and *Dinophysis acuminata*, on the survival, growth, and swimming activity of early life stages of forage fish. Mar Environ Res 148:46–56
Rourke WA, Murphy CJ, Pitcher G, van de Riet JM, Burns BG, Thomas KM, Quilliam MA (2008) Rapid postcolumn methodology for determination of paralytic shellfish toxins in shellfish tissue. J AOAC Int 91:589–597
Smayda TJ, Reynolds CS (2001) Community assembly in marine phytoplankton: application of recent models to harmful dinoflagellate blooms. J Plankton Res 23:447–461
Sun J, Liu DY (2003) Geometric models for calculating cell biovolume and surface area for phytoplankton. J Plankton Res 25:1331–1346

Taylor FJR (1987) The biology of dinoflagellates. Botanical Monographs, Book 21. Blackwell & University of California Press

Tong MM, Kulis DM, Fux E, Smith JL, Hess P, Zhou QX, Anderson DM (2011) The effects of growth phase and light intensity on toxin production by *Dinophysis acuminata* from the northeastern United States. Harmful Algae 10:254–264

Trainer VL, Pitcher GC, Reguera B, Smayda TJ (2010) The distribution and impacts of harmful algal bloom species in eastern boundary upwelling systems. Prog Oceanogr 85:33–52

Vale P, Botelho MJ, Rodrigues SM, Gomes SS, Sampayo MAM (2008) Two decades of marine biotoxin monitoring in bivalves from Portugal (1986–2006): a review of exposure assessment. Harmful Algae 7:11–25

Velo-Suarez L, González-Gil S, Pazos Y, Reguera B (2014) The growth season of *Dinophysis acuminata* in an upwelling system embayment: a conceptual model based on *in situ* measurements. Deep Sea Res II 101:141–151

von Stosch HA (1973) Observations on vegetative reproduction and sexual life cycles of two freshwater dinoflagellates, *Gymondinium pseudopalustre* Schiller and *Woloszynskia apiculata* sp. nov. Eur J Phycol 8:105–134

Wardhani DH, Vazquez JA, Pandiella SS (2010) Optimisation of antioxidants extraction from soybeans fermented by *Aspergillus oryzae.* Food Chem 118:731–739

Wyatt T (2014) Margalef's mandala and phytoplankton bloom strategies. Deep Sea Res II 101:32–49

Wyatt T, Zingone A (2014) Population dynamics of red tide dinoflagellates. Deep Sea Res II 101:231–236

Zingone A, Escalera L, Aligizaki K, Fernandez-Tejedor M and others (2021) Toxic marine microalgae and noxious blooms in the Mediterranean Sea: a contribution to the Global HAB Status Report. Harmful Algae 102: 101843

Editorial responsibility: Ilana Berman-Frank, Haifa, Israel
Reviewed by: 2 anonymous referees

Submitted: May 9, 2022
Accepted: January 11, 2023
Proofs received from author(s): March 2, 2023